Lithos 262 (2016) 135–152

Contents lists available at ScienceDirect

Lithos

journal homepage: www.elsevier.com/locate/lithos

Subduction zone mantle enrichment by fluids and Zr–Hf-depleted crustal melts as indicated by backarc basalts of the Southern Volcanic Zone, Argentina

Paul M. Holm [a,*], Nina Søager [a,b], Mads Alfastsen [a], Gustavo W. Bertotto [c]

[a] Department of Geosciences and Natural Resource Management, University of Copenhagen, Øster Voldgade 10, DK-1350 Copenhagen, Denmark
[b] GEOMAR, Helmholtz Centre for Ocean Research, D-24148 Kiel, Germany
[c] INCITAP, CONICET-National University of La Pampa, Avenida Uruguay 151, Santa Rosa, Argentina

ARTICLE INFO

Article history:
Received 19 April 2016
Accepted 29 June 2016
Available online 07 July 2016

Keywords:
Andean volcanism
Southern Volcanic Zone
Mantle enrichment
Geochemical modelling

ABSTRACT

We aim to identify the components metasomatizing the mantle above the subducting Nazca plate under part of the Andean Southern Volcanic Zone (SVZ). We present new major and ICP-MS trace element and Sr, Nd and high-precision Pb isotope analyses of primitive olivine-phyric alkali basalts from the Northern Segment Volcanic Field, part of the Payenia province in the backarc of the Transitional SVZ. One new ^{40}Ar–^{39}Ar age determination confirms the Late Pleistocene age of this most northerly part of the province. All analysed rocks have typical subduction zone type incompatible element enrichment, and the rocks of the Northern Segment, together with the neighbouring Nevado Volcanic Field, have isotopic compositions intermediate between adjacent Transitional SVZ arc rocks and southern Payenia OIB-type basaltic rocks. Modelling the Ba–Th–Sm variation we demonstrate that fluids as well as 1–2% melts of upper continental crust (UCC) enriched their mantle sources, and La–Nb–Sm variations additionally indicate that the pre-metasomatic sources ranged from strongly depleted to undepleted mantle. Low Eu/Eu* and Sr/Nd also show evidence for a UCC component in the source. The contribution of Chile Trench sediments to the magmas seems insignificant. The Zr/Sm and Hf/Sm ratios are relatively low in many of the Northern Segment rocks, ranging down to 17 and 0.45, respectively, which, together with relatively high Th/U, is argued to indicate that the metasomatizing crustal melts were derived by partial melting of subducted UCC that had residual zircon, in contrast to the UCC melts added to Transitional SVZ arc magmas. Mixing between depleted and undepleted mantle, enriched by UCC and fluids, is suggested by Sr, Nd and Pb isotopes of the Northern Segment and Nevado magmas. The metasomatized undepleted mantle south of the Northern Segment is suggested to be part of upwelling OIB-type mantle, whereas the pre-metasomatically depleted mantle also can be found as a component in some arc rocks. The fluid-borne enrichment seems to have been derived from South Atlantic wedge mantle with no significant transfer of solubles in the slab fluids from the subducting altered Pacific oceanic crust to the wedge. The Northern Segment magmatism is proposed to be related to the steepening of Nazca plate subduction in the Pleistocene after a shallow slab period, where melts of subducted UCC plus slab fluids metasomatized the overlying depleted wedge mantle. During this steepening, the enriched depleted and undepleted mantle mixed or interacted, and yielded the Northern Segment and Nevado magmas.

1. Introduction

There is a general consensus that subduction zone volcanism is related to the interaction of subducted materials with the overlying mantle wedge, but which materials interact, and how, is much more debated (e.g. Holm et al., 2014; Jacques et al., 2013; Kay et al., 2006; Marshall and Schumacher, 2012; Spandler et al., 2014; Straub et al., 2011; Völker et al., 2014). In the Southern Volcanic Zone (SVZ) of the Andes, the relative contribution to the magmas of subducted upper continental crust (UCC), sediments, and altered oceanic crust has recently been discussed (e.g. Holm et al., 2014; Jacques et al., 2013; Kay et al., 2004; Stern, 2004). In the Payenia backarc province of the SVZ, Pleistocene alkaline magmas that have typical subduction zone incompatible element enrichment erupted in the northern part contemporaneously with OIB-type enriched alkaline magmas in the southern part. These alkaline rocks are believed to have been formed over a steepening subducting Nazca plate after a period of shallow subduction during

* Corresponding author.
E-mail address: paulmh@ign.ku.dk (P.M. Holm).

http://dx.doi.org/10.1016/j.lithos.2016.06.029
0024-4937/

the late Miocene and Pliocene (e.g. Bermúdez et al., 1993; Bertotto et al., 2009; Gudnason et al., 2012; Kay et al., 2004, 2013; Søager and Holm, 2013; Søager et al., 2013, 2015a). In this paper we attempt to explain the origin of the subduction zone enriched alkaline rocks based on new geochemical data from the northernmost volcanic field in the Payenia backarc, the Northern Segment. We also demonstrate an important role of melts of subducted upper continental crust in the enrichment of the mantle sources of the Northern Segment magmas.

Søager et al. (2015a) showed that the northern Payenia volcanism just south of the Northern Segment was derived from mantle enriched by 1–2% UCC and fluids. This is similar to what was found for the adjacent arc volcanic rocks of the Transitional SVZ (TSVZ) by Holm et al. (2014), but the pre-metasomatic backarc mantle was often less depleted than the pre-metasomatic arc mantle (Søager et al., 2015a). Here we discuss the relative mantle enrichment by fluids and UCC, respectively, and demonstrate that for the Northern Segment, the enriching crustal melts were distinct from those of most of the arc mantle in general. Because of the distinctly different isotopic composition of Pacific and South Atlantic MORB, it is possible to detect that the SVZ arc and backarc magmas consistently lack Pb and Sr isotopic evidence for contribution from subducted altered Pacific oceanic crust. We suggest that the Pb and Sr in the fluids originate from leaching of the wedge mantle rather than from the slab. Finally, in the context of Pliocene-Pleistocene changes in the steepness of the subducting Nazca plate, we discuss the cause for the occurrence of three types of magma in the TSVZ arc and backarc: frontal arc calc-alkaline magmas, backarc alkaline OIB-type magmas, and alkaline magmas with subduction zone type enrichment.

2. Geology of the Northern Segment

The Northern Segment is the northernmost part of the Payenia backarc province (Fig. 1) situated east of the TSVZ and NSVZ. Its northern limit coincides with the tectonic change from normal subduction to the Pampean flat slab (Folguera et al., 2009; Gudnason et al., 2012; Kay et al., 2006). Gudnason et al. (2012) elaborating on the scenario of Folguera et al. (2009) suggested a temporal gradual progression of backarc volcanism with subduction zone enriched alkaline magmas from the southern part of the Nevado volcanic field in Late Pliocene (2.8–0.8 Ma) to the Northern Segment in the Late Pleistocene. Also the OIB-type volcanism progressed northwards in the Pleistocene from Auca Mahuida via Río Colorado to Payún Matrú and Llancanelo (Kay et al., 2013; Søager and Holm, 2013). A compressional tectonic regime in the Late Miocene and Pliocene associated with a shallowly subducting slab was released by Quaternary extensional collapse of the foreland region (Folguera et al., 2009; Ramos et al., 2014) but no backarc rifting occurred.

The Quaternary rocks of Northern Segment (Folguera et al., 2009; Gudnason et al., 2012) are wedged between the Andean foothills to the west and the eastern thrust faults of the San Rafael block to the east (Fig. 1). The volcanic rocks are basaltic and occur north of Río Atuel and the volcanic fields of Nevado and Llancanelo, and stretch north for around 100 km to just SE of Pareditas (Fig. 1b and c). In the Northern Segment there is one composite volcano and a number of volcanic clusters consisting of mainly monogenetic cones, most of which have been sampled in this study. The morphologies range from purely pyroclastic cones to effusive eruptive centres, the exception being the 1 km high stratocone of Cerro (Co.) Diamante, which overlies some of the Neogene remnants of volcanism (Folguera et al., 2009) not dealt with in this work. Volcanism took place in the Middle to Late Pleistocene approximately in the interval 0.7–0.06 Ma (Dyhr et al., 2013a; Folguera et al., 2009; Gudnason et al., 2012) with no clear geographical correlation of ages (Fig. 1c).

The Northern Segment volcanoes may be subdivided into 8 groups based mostly on the clustering of eruptive centres: Huaiquería (with Guadal), Papagayos, Rodeo, Loma del Medio (with Co. Arroyo Hondo), Co. Diamante, Las Bolas, La Leña and Los Reyunos (Agua del Toro, Galileo Vitale, Co. Negro de las Salinas) (Fig. 1c), and deviates slightly from that of Folguera et al. (2009). Additional information of the geology of the Northern Segment, locations and petrographic information of the samples are presented in Supplementary data A.

3. Analytical procedures

Forty-three petrographically fresh samples considered relatively unaltered were jaw crushed and subsequently powdered in an agate mill. Major elements were analysed at the Acme Analytical Laboratories Ltd., Canada (Acme Labs; Code 4A) by fusion of the samples into glass and analysis by ICP-AES. Volatile contents were estimated by loss on ignition at 1000 °C. ICP-MS analysis was carried out on dissolutions of the samples on a PerkinElmer 6100 DRC Quadrupole at GEUS (Geological Survey of Denmark and Greenland). Reproducibility of the standards in the period of analyses is 3–4 rel.% (2σ, $n = 45$) for most elements and incompatible element ratios used in this work including Eu/Eu*. Abundances of all incompatible elements discussed in this paper deviate less from the GeoReM preferred Values (Jochum and Nehring, 2006) than the 2σ uncertainty. Some samples were duplicated to check completeness of dissolution and sample homogeneity. With special reference to Zr, a selection of elements were additionally analysed (1) by XRF and (2) by ICP-MS after borate melting to test total dissolution by HF in the standard preparation for ICP-MS. No difference between results from XRF and the two preparations for ICP-MS could be detected for the selected elements including Zr. Documentation for the quality of the analytical data is presented in Supplementary data B.

Eighteen of the samples were analysed for Pb, Sr and Nd isotopic compositions. Unaltered chips were picked from the jaw crushed material and leached in 6 N HCl for 1 h at 130 °C. Mass spectrometric analyses of separated Sr, Nd and Pb were performed on a VG 54-30 MC-TIMS in the Department of Geosciences and Natural Resource Management, University of Copenhagen. Sr isotope results of international standard NBS987 run around the period of sample analysis yielded: $^{87}Sr/^{86}Sr = 0.710241 \pm 0.000019$ (2σ, $n = 60$). The reproducibility of the international standard JNdi was: $^{143}Nd/^{144}Nd = 0.512096 \pm 0.000016$ (2σ, $n = 53$). Pb was run according to the $^{207}Pb/^{204}Pb$ double-spike method (Baker et al., 2004). Spiking and loading on Re-filaments were done as described by Thirlwall (2000). Samples of around 50 ng Pb were all analysed at temperatures of 1200–1250 °C. The international standard NBS981 reproduced thus: $^{206}Pb/^{204}Pb = 16.9391 \pm 0.0030$, $^{207}Pb/^{204}Pb = 15.4988 \pm 0.0034$ and $^{208}Pb/^{204}Pb = 36.7243 \pm 0.0090$ (2σ, $n = 13$). All blanks were below 200 pg Pb, which is insignificant considering the amount of sample Pb available for analysis.

For ^{40}Ar–^{39}Ar age analysis, the groundmass of La Leña sample 126086 was separated from a 0.2–0.3 mm sieve fraction of jaw crushed rock using magnetic susceptibility differences and by hand picking. Two splits of the sample were analysed on a Micromass 5400 mass spectrometer at Lund University, Sweden. The age results are presented in Table 1, and the analytical data in Supplementary data C.

4. Results

4.1. Age of La Leña volcano

One sample split yielded an age plateau of all the released argon with an age of 0.46 ± 0.08 Ma (2σ) and a MSWD of 0.6 (Table 1). A less precise isochron age and the integrated age of all argon support the preferred plateau age. The second split did not yield an age plateau but both an isochron age and the integrated age are in accord with the plateau age of the first split. This age of the most southwesterly volcano of the Northern Segment is comparable to the age of the lava of Agua del Toro (Los Reyunos group), volcanism at Co. Arroyo Hondo (Loma del Medio group) (Fig. 1c) and Co. Guadal (Huaiquería group), the most northerly edifice, and confirm that no simple geographically related

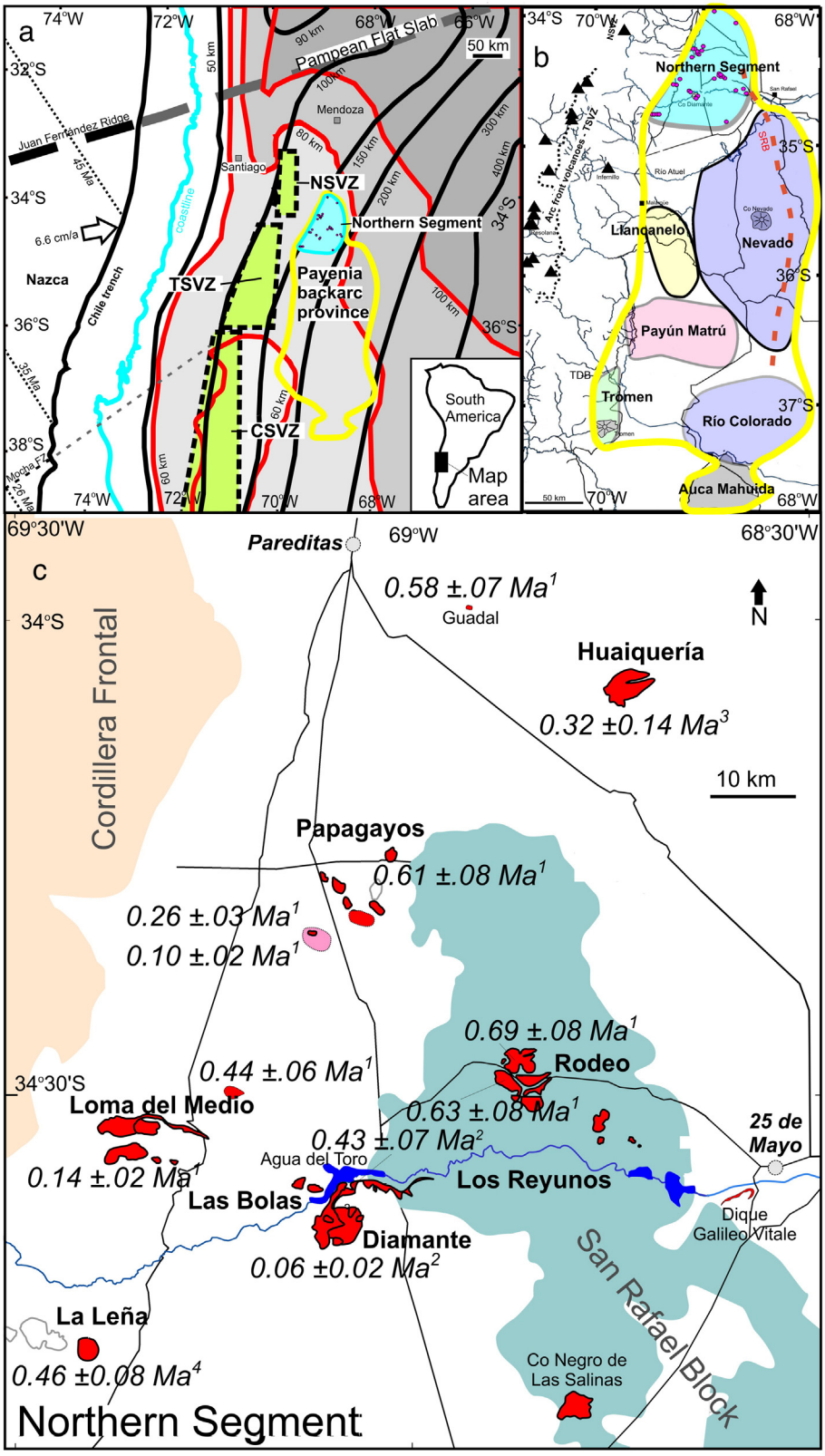

Fig. 1. Maps. a) South American and Nazca lithospheric plates with positions of the Payenia backarc province (yellow line) with the Northern Segment volcanic field (in blue) and Northern, Transitional and Central Southern Volcanic Zones (NSVZ, TSVZ, CSVZ) (in green). Thick black lines: Chile trench and Nazca slab depth contours, red lines: lithosphere thickness and slab depth contours (Tassara et al., 2006), seafloor ages: Tebbens and Cande (1997). Ages of magnetic anomalies on the Nazca plate, the Juan Fernández hotspot trace and the Mocha fracture zone are indicated. Arrow: direction and speed of net plate convergence (Kendrick et al., 2003). Modified from Holm et al. (2014). b) Payenia volcanic fields (Gudnason et al., 2012; Søager et al., 2013). Also shown are Arc front volcanoes of TSVZ, the red stippled lines mark the eastern late Miocene thrust fronts, and SRB: the San Rafael Block west of red stipple (also in c). Dotted line: national border. c) The Northern Segment volcanic field of the Payenia backarc province. Ages of volcanic rocks are given with 2σ errors: 1 — Folguera et al. (2009) K–Ar, 2 — Gudnason et al. (2012) ^{40}Ar–^{39}Ar, 3 — Dyhr et al. (2013a) ^{40}Ar–^{39}Ar, 4 – La Leña – this work. Basement outcrops of the SRB in blue after Ramos et al. (2014). (For interpretation of the references to colour in this figure legend, the reader is referred to the web version of this article.)

Table 1
^{40}Ar–^{39}Ar analyses of Cerro La Leña, Northern Segment volcanic field, Payénia backarc province, Andean Southern Volcanic Zone, Mendoza, Argentina.

Location	Sample no.	Analysis no.	Plateau				Isochron			Integrated age	Geographical position	
			Age ± 2σ Ma	N/N^{tot}	^{39}Ar (%)	MSWD	Age ± 2σ Ma	$^{40}Ar/^{36}Ar$	MSWD	Age ± 2σ Ma	°S	°W
Co. La Leña	126085	2382-01	0.46 ± 0.08	7/7	100	0.6	0.4 ± 0.2	300 ± 20	0.6	0.44 ± 0.09	34.764	69.421
		2382-02		No plateau			0.5 ± 0.3	320 ± 50	0.6	0.47 ± 0.10		

Underlined: preferred age result.

age progression is indicated within this volcanic field, which seems to be entirely erupted during Middle–Late Pleistocene (Fig. 1c).

4.2. Geochemical data

All Northern Segment samples are relatively primitive alkali basalts with 6.3–14.5 wt.% MgO, Mg# 59–76, and Ni up to 350 ppm (Table 2, Fig. 2a and b, Supplementary data D). This is similar to the basalts of the Nevado and Llancanelo volcanic fields, whereas samples from Río Colorado and Payún Matrú volcanic fields in southern Payenia are mostly trachybasalts (Germa et al., 2010; Hernando et al., 2012; Kay et al., 2013; Søager and Holm, 2013; Søager et al., 2013). In this paper we compare the new data only to other samples with Mg# ≥ 58 to avoid effects of extensive fractional crystallization. Compared to the OIB-type magmas of Río Colorado and Payún Matrú, the Northern Segment, as well as Nevado and Llancanelo, have lower High Field Strength Element (HFSE) concentrations, e.g. TiO_2 and Nb, but higher concentrations of these than in frontal arc magmas of the SVZ (Fig. 2c and d).

The Northern Segment rocks have an enrichment in Large Ion Lithophile Elements (LILEs) and Light Rare Earth Elements (LREEs) relative to the HFSEs Nb, Ta and Ti, and have similar incompatible element patterns to arc rocks in general (e.g. Tatsumi and Kogiso, 2003). The patterns also largely conform to SVZ frontal arc rocks, but Northern Segment rocks have higher abundances of less incompatible elements and Nb–Ta (Fig. 2f). Northern Segment rocks contrast to the Río Colorado and Payún Matrú rocks, which have typical OIB-type incompatible element patterns without negative anomalies for Nb, Ta and Ti and no positive Pb anomaly. A strong LREE/HFSE enrichment of the Northern Segment magmas in several cases exceeds that of adjacent Nevado volcanic rocks and in some Rodeo and Papagayos rocks reach La/Nb = 3.7, comparable to many TSVZ magmas.

For both of the largest volcanic clusters in the Northern Segment, the rocks display significant variation in trace element ratios. In the Papagayos group, there is a N–S increase of La/Nb from 2 to 3, whereas in the Rodeo group, the variation is from 1.8 for Co. Rodeo and Chico, via 2.5 in La Chilena and Loma del Medio, to 3.5 in Co. Chato and edifice "1784m" (see maps in Supplementary data A). The Ba/Th ratio for the two clusters shows a similar relative variation, which is comparable to the variation of the entire Northern Segment.

Our comparison of Northern Segment rocks with other Payenia rocks is limited to the least contaminated compositions according to criteria discussed by Søager et al. (2013) and Søager and Holm (2013) with respect to lower crustal contamination. For Nevado this includes rocks with Ba/Th < 125 and for Río Colorado, Payún Matrú and Llancanelo rocks with Ba/Th < 210 and Ba/Nb < 17. Based on these criteria none of the Northern Segment magmas are expected to be contaminated with lower continental rocks as found elsewhere in Payenia.

Nd and Sr isotopic compositions of the Northern Segment basalts (Table 3) overlap with Transitional and Central SVZ arc as well as with other backarc rocks (Fig. 3a). T-CSVZ rocks and southern backarc intraplate rocks do not overlap in Pb isotopic compositions (Fig. 3b–d), but Pb isotope compositions for the Northern Segment span the gap and range from relatively unradiogenic SVZ arc samples to the radiogenic end of the field of Llancanelo rocks (Fig. 3b). The Northern Segment extends the isotopic variation displayed by Nevado with which it overlaps.

5. Discussion

The majority of the Northern Segment samples can be modelled by fractionation of less than 10% olivine (+ minor chromite) from primitive magmas with 10–12 wt.% MgO and Mg# around 72 (Fig. 2b) which would be in equilibrium with typical mantle olivine of $Fo_{89–90}$. High Mg# > 72 in some rocks from Papagayos and Rodeo having 10–20% olivine phenocrysts may be explained by accumulation of up to c. 7% olivine (Fig. 2b). No fractionation of clinopyroxene, plagioclase or Fe-Ti oxide in the erupted magmas is indicated by major and compatible trace elements. For instance, with decreasing MgO, no significant change is observed in or between groups of element ratios sensitive to fractionation of these phases, such as CaO/Al_2O_3, Al_2O_3/TiO_2, V/Sc (Fig. 2e), or Sr/Nd (Fig. 4a). The presence of plagioclase and/or clinopyroxene phenocrysts in a number of these rocks, therefore, does not seem to indicate fractionation of these phases. Thus, Northern Segment rocks generally have compositions which may be good approximations to mantle melts.

Contamination with upper continental crust would be expected to be noticeable in particular by a change in geochemical parameters that are typically distinctly different in UCC and mantle melts such as Ba/Th, Sr/Nd and Eu/Eu* which are all relatively low in UCC. Often contamination of magmas take place as part of an AFC process (DePaolo, 1981) and therefore magmatic evolution may be accompanied by a decrease of these ratios. However, the variation in Fig. 4 clearly lacks any indication that AFC type processes were important during the magmatic evolution of the Northern Segment magmas, as there is no significant correlation between these ratios and MgO. In the diagram also contamination with lower continental crust is confirmed not to be important.

5.1. Source enrichment by hydrous fluid vs. continental crust

LILEs such as Ba and Sr have been proven to be more soluble in hydrous fluids than the LREE, whereas the HFSEs Nb and Ta and middle-heavy REEs (Sm-Lu) are much less soluble, and the highly charged, but large, Th ion intermediately to little soluble (e.g. Brenan et al., 1995; Kessel et al., 2005; Kogiso et al., 1997; Xiao et al., 2012). At high temperatures and pressures, these differences diminish, and as hydrous fluids become supercritical at pressures around 6 GPa, their trace element affinities become like silicate melts (Kessel et al., 2005). The upper continental crust (UCC) is dominated by granite and evolved, to a large extent, by intracrustal magmatic differentiation (Rudnick and Gao, 2003; Taylor and McLennan, 1985). Because such highly evolved magmas have fractionated plagioclase and alkali feldspar, they tend to have relatively low Ba/Th, Sr/Nd, and Eu/Eu*. Therefore, they have a geochemical contrast to hydrous fluids with higher ratios. We first investigate the variation of the Ba/Th ratio in the Northern Segment rocks to test the possible effects from metasomatism of their source mantle by UCC or fluids, because enrichment by both were found to be significant in the SVZ frontal arc magmas (Holm et al., 2014).

Table 2
Major and trace element composition of representative samples from the Northern Segment Volcanic Field of Payénia backarc province, Andean Southern Volcanic Zone, Mendoza, Argentina[1].

Group/Volcano	Huaiquería group			Papagayos group				Rodeo group			Diamante group			L d Medio	La Leña	Los Reyunos group	
Edifice/unit	Guadal	Huaique-ría Lava C	Huaiquería Scoria II	Co Los Leones	Co del Medio	Co Los Leones	Co Guadaloso	Co. Rodeo	Co. "1784"	Co. la Chilena	Co. Dia-mante	Las Bolas NW cone	Co Negra deSalinas		Co. La Leña	Agua del Toro	Galileo Vitale
Latitude (degrees)	−33.9871	−34.0697	−34.0772	−34.2503	−34.2785	−34.2505	−34.3110	−34.4692	−34.4785	−34.4934	−34.6378	−34.5872	−34.8180	−34.5403	−34.7642	−34.5923	−34.5935
Longitude (degrees)	−68.9274	−68.7543	−68.7434	−69.0282	−69.0944	−69.0251	−69.0652	−68.8693	−68.8604	−68.8265	−69.0848	−69.1416	−68.8150	−69.2658	−69.4210	−69.0310	−68.5571
Sample#	127312	127318	127323	126051	127311	127424	127310	126078	126077	127327	123964	127437	127001	126083	126085	123965	127307
Approximate age[3]	530 ka	320 ka		610 ka				650 ka			60 ka			140 ka	460 ka	430 ka	
SiO_2 − wt.%[2]	49.74	45.67	45.53	45.97	45.27	45.93	44.99	47.48	45.39	47.40	48.40	47.80	45.51	48.88	47.48	48.38	48.21
TiO_2	1.40	1.46	1.41	1.51	1.38	1.56	1.18	1.58	1.34	1.44	1.71	1.44	1.43	1.32	1.81	1.57	1.43
Al_2O_3	15.95	15.38	14.88	15.28	15.29	15.81	13.73	14.87	15.24	15.72	16.53	16.02	15.77	15.43	17.19	14.97	15.02
$Fe_2O_3^{total}$	9.38	10.64	10.88	10.85	11.17	11.30	11.35	11.19	11.81	10.87	11.47	11.13	10.90	10.13	10.97	11.67	11.28
MnO	0.17	0.19	0.19	0.18	0.18	0.18	0.17	0.17	0.20	0.18	0.16	0.18	0.17	0.17	0.18	0.16	0.16
MgO	6.72	10.49	10.06	11.20	10.87	11.01	14.48	6.67	11.28	8.77	6.54	9.50	9.38	9.46	6.79	9.84	10.03
CaO	11.44	11.13	11.88	10.56	11.54	11.21	10.90	12.12	11.05	11.10	10.62	11.15	12.27	10.20	10.70	9.36	10.05
Na_2O	3.50	3.11	3.24	3.41	2.98	3.15	2.14	3.04	2.31	3.04	3.52	2.99	3.28	2.90	3.14	3.18	3.01
K_2O	1.64	1.42	1.41	0.72	1.07	1.42	0.97	1.34	0.98	1.24	1.03	1.17	1.13	1.36	1.62	1.07	1.01
P_2O_5	0.46	0.82	0.85	0.54	0.49	0.57	0.36	0.56	0.56	0.47	0.43	0.38	0.47	0.46	0.57	0.34	0.34
Volatiles	2.6	0.5	2.2	0.8	1.1	0.9	1.9	3.9	1.2	0.2	−0.3	1.0	1.7	0.7	0.3	−0.1	0.8
	99.65	99.46	99.45	99.44	99.53	101.11	99.42	99.54	99.50	99.53	99.49	100.85	99.49	99.51	99.56	99.61	99.65
Mg# ($Fe^{2+}/Fe^{tot} = 0.8$)	64.0	70.9	69.6	71.9	70.7	70.7	76.0	59.6	70.3	66.6	64.7	67.9	68.1	69.8	60.5	67.6	68.8
Sc − ppm	27.59	30.94	24.47	30.24	24.27	31.38	29.94	28.08	27.35	31.70	38.22	30.55	26.88	29.25	31.11	24.08	29.26
V	256.78	262.94	215.64	272.82	213.02	264.73	257.08	233.53	230.64	280.06	297.18	257.40	237.00	249.94	290.23	206.47	231.62
Cr	192.08	375.37	341.84	402.09	438.94	420.61	796.31	496.42	508.20	281.36	202.91	338.92	297.94	358.16	120.42	393.94	413.61
Mn	1280	1480	1291	1359	1203	1407	1331	1245	1484	1335	1232	1360	1230	1267	1402	1268	1312
Co	35.92	46.33	39.37	46.29	40.47	46.90	55.76	48.37	49.52	40.01	37.37	44.56	43.18	42.27	37.37	49.12	52.63
Ni	74.62	184.03	174.36	206.94	186.43	201.85	335.65	249.51	239.64	97.67	57.72	151.74	167.51	152.73	49.59	207.08	200.04
Cu	51.19	56.24	54.01	47.58	60.11	64.90	67.13	51.97	35.93	64.09	57.49	56.81	41.17	69.86	60.72	50.49	47.15
Zn	62.74	74.95	67.24	75.75	64.42	80.75	68.51	73.09	75.65	77.78	71.98	77.24	73.84	64.63	71.01	84.21	89.41
Ga	21.18	19.06	16.71	19.22	15.98	20.11	16.22	18.65	20.14	20.58	20.38	19.49	18.18	19.81	21.11	19.38	19.24
Rb	47.37	33.74	18.23	28.33	14.86	30.63	16.95	23.11	25.17	28.41	26.07	25.12	23.25	26.90	31.15	23.37	23.16
Sr	986	1209.60	1004	868	662	837	858	851	992	949	705	645	753	873	893	617	544.30
Y	20.47	28.92	26.02	23.94	17.82	23.69	18.40	22.23	23.64	21.37	20.01	21.27	22.55	21.56	25.98	21.86	22.88
Zr	140.72	171.22	150.89	148.06	102.60	146.80	95.25	135.32	138.89	128.43	114.32	117.65	115.53	134.58	147.71	115.15	112.19
Nb	17.36	20.40	18.11	16.39	9.48	16.49	7.77	12.76	10.99	11.77	11.21	9.27	13.13	10.92	15.12	10.48	11.52
Cs	1.57	2.34	2.74	1.67	0.75	1.58	0.82	0.57	1.36	1.04	1.15	0.88	1.06	1.36	1.54	0.65	0.68
Ba	681	776.75	723	532	397	563	454	480	607	616	495	473	562	597	632	352	415.85
La	25.86	40.34	36.91	35.26	24.40	35.69	21.60	23.25	38.32	27.42	24.85	20.89	26.67	25.33	28.15	17.04	18.28
Ce	52.86	80.57	70.12	71.07	47.38	72.62	44.35	48.29	77.47	54.42	49.96	44.17	52.45	51.86	57.10	35.91	37.24
Pr	6.89	10.08	9.18	8.50	6.30	9.17	6.19	6.49	9.94	7.18	6.24	5.74	5.83	6.89	7.59	4.63	4.82
Nd	27.96	40.94	36.44	34.95	25.57	36.47	25.74	27.08	40.62	28.96	25.69	24.03	24.30	28.33	31.57	19.93	20.97
Sm	5.79	8.14	7.24	6.99	5.26	7.36	5.37	5.67	7.64	5.78	5.13	5.09	4.99	5.68	6.40	4.65	4.71
Eu	1.64	2.38	2.03	1.98	1.45	2.08	1.49	1.67	2.18	1.66	1.64	1.55	1.64	1.68	1.86	1.54	1.50
Gd	5.19	7.59	6.79	6.19	4.82	6.85	4.99	5.43	6.80	5.43	5.18	5.04	5.14	5.24	5.96	4.92	4.69
Tb	0.735	1.056	0.950	0.855	0.675	0.911	0.692	0.785	0.925	0.755	0.711	0.722	0.740	0.757	0.891	0.716	0.746
Dy	3.77	5.34	5.01	4.48	3.54	4.96	3.71	4.24	4.65	4.11	3.95	4.13	4.17	4.16	4.82	3.95	4.17
Ho	0.719	1.037	0.937	0.808	0.649	0.848	0.680	0.805	0.830	0.772	0.721	0.763	0.800	0.779	0.904	0.776	0.823
Er	1.90	2.72	2.56	2.14	1.70	2.27	1.77	2.16	2.20	2.05	1.90	2.07	2.13	2.07	2.51	2.08	2.23
Tm	0.265	0.425	0.352	0.295	0.229	0.310	0.249	0.301	0.292	0.273	0.253	0.295	0.310	0.309	0.348	0.282	0.312
Yb	1.57	2.52	2.16	1.80	1.37	1.82	1.42	1.86	1.81	1.68	1.60	1.83	1.84	1.76	2.19	1.79	1.96
Lu	0.237	0.383	0.332	0.259	0.206	0.274	0.204	0.279	0.263	0.247	0.232	0.268	0.290	0.272	0.333	0.260	0.295
Hf	3.52	4.11	3.44	3.37	2.52	3.67	2.57	3.26	3.67	3.11	3.01	3.03	2.84	3.43	3.61	2.77	2.86
Ta	0.895	1.088	0.961	0.902	0.520	0.914	0.440	0.713	0.599	0.654	0.625	0.506	0.670	0.621	0.868	0.595	0.630
Pb	12.08	11.39	8.76	7.18	4.81	7.73	4.60	5.12	11.45	9.33	7.26	6.76	7.13	10.08	7.62	5.08	6.69
Th	5.96	8.20	8.05	6.77	5.00	7.46	4.94	4.39	8.83	6.32	5.72	4.30	5.16	5.76	5.76	3.12	3.36
U	2.66	2.23	2.14	1.45	0.97	1.48	0.94	0.98	1.66	1.33	1.21	1.22	1.38	1.48	1.43	0.88	0.70

1 — See Supplementary information C for the full data set. 2 — Recalculated on a volatile free basis and $Fe^{2+}/Fetot = 0.8$. Volatiles were measured by loss on ignition. 3 — Based on available age data (see Fig. 1c).

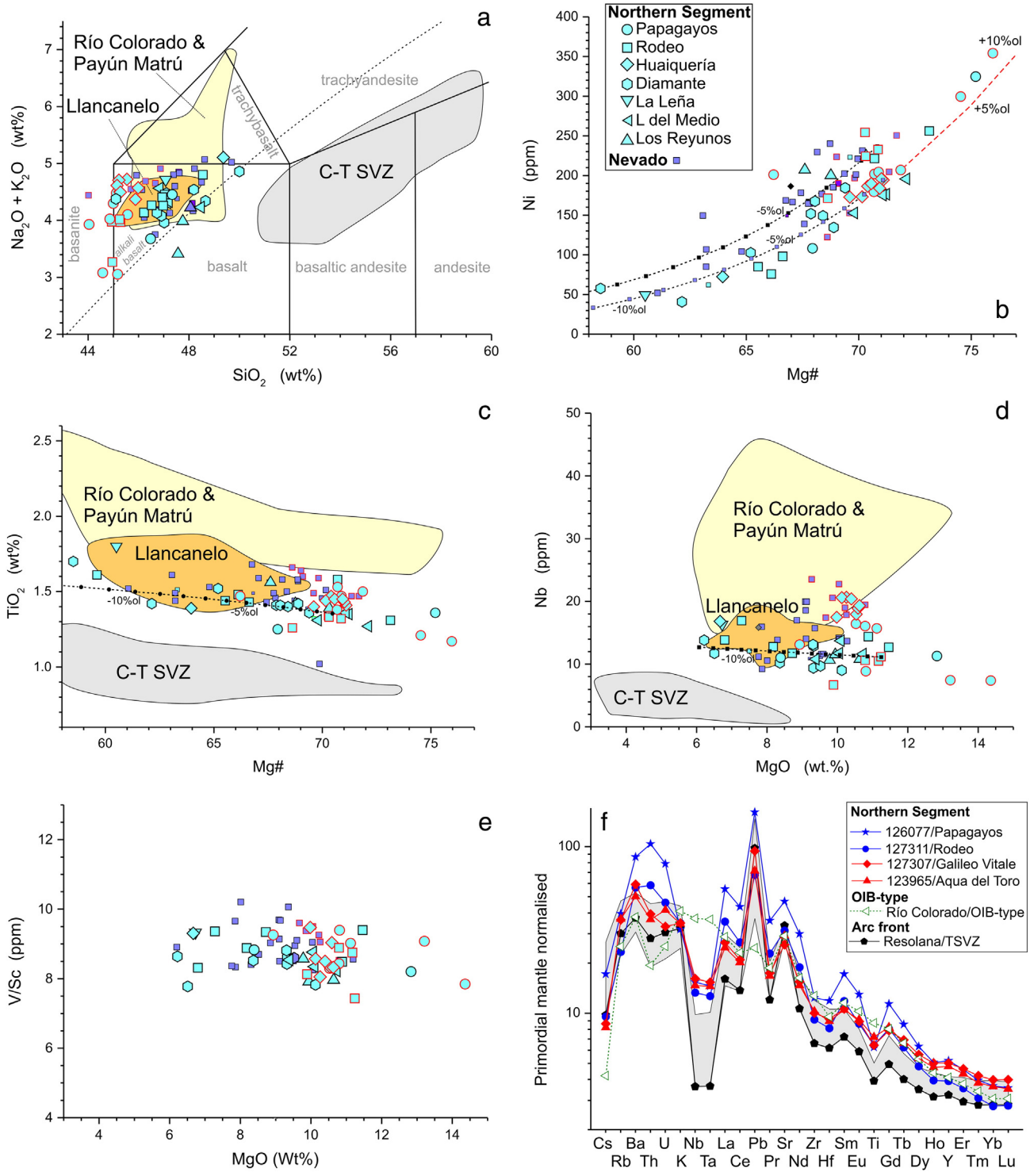

Fig. 2. Geochemical variation of samples from the Northern Segment and Nevado volcanic fields of Payenia backarc province. a) TAS diagram, b) Ni vs. Mg#, c) TiO_2 vs. Mg#, d) Nb vs MgO, e) V/Sc vs. MgO, f) incompatible element patterns. For comparison are shown the compositions of the Río Colorado plus Payún Matrú volcanic fields (of OIB type rocks), the Llancanelo volcanic field of Payenia, and the adjacent part of the Central-Transitional SVZ of the frontal arc. For the new data from the Northern Segment, the shape of symbol designate volcano group (see legend in b). Red outline of symbols: rocks with relatively low Zr and Hf. Stippled line in a approximately separates silica undersaturated and saturated compositions. Dotted lines in b and c are examples of calculated olivine fractionation trends with tick marks for each percent, and the dashed red line in b shows the calculated effect of accumulation of olivine. PM (Sun and McDonough, 1989) normalized concentrations in f are for representative samples from the Northern Segment, one OIB-type Río Colorado sample 124564 (Søager et al., 2015a) and arc sample CL741 from Resolana at Co. Azul in the TSVZ (Jacques et al., 2013). The shaded area encompasses variation within TSVZ. Stippled line is division of subalkaline and alkaline volcanic rocks (Irvine and Baragar, 1971). (For interpretation of the references to colour in this figure legend, the reader is referred to the web version of this article.)
Data sources: Jacques et al. (2013); Holm et al. (2014); Søager et al. (2013, 2015a); Søager and Holm (2013).

The Northern Segment rocks display enrichments of Th and Ba relative to Sm comparable to SVZ frontal arc rocks (Fig. 5a). We use Sm because it is much less fluid mobile than the lightest REEs and therefore useful in the evaluation of a fluid-borne source enrichment of e.g. Ba. Also, Sm is not as enriched in crustal rocks as the most incompatible REEs and e.g. Th. Because Sm is less incompatible than e.g. La, Th and

Table 3
Isotopic composition of Nd, Sr and Pb in volcanic rocks of the Northern Segment volcanic field of the Payenia backarc volcanic province, Southern Volcanic Zone, Mendoza, Argentina.

Group/volcano	Edifice/unit	Sample id	$^{143}Nd/^{144}Nd$	$\pm 1\sigma^{1}(*10^{6})$	$^{87}Sr/^{86}Sr$	$\pm 1\sigma^{1}(*10^{6})$	$^{206}Pb/^{204}Pb$	$\pm 1\sigma^{2}(*10^{4})$	$^{207}Pb/^{204}Pb$	$\pm 1\sigma^{2}(*10^{4})$	$^{208}Pb/^{204}Pb$	$\pm 1\sigma^{2}(*10^{4})$
Huaiquería group	Guadal volcano	127312	0.512820	4	0.703975	4	18.5765	13	15.6041	16	38.4890	50
	Huaiquería volcano, Lava C	127318	0.512826	4	0.704083	4	18.5605	11	15.5935	13	38.4410	41
		Duplicate	0.512829	3								
	Huaiquería volcano, Scoria II	127320	0.512811	5	0.704017	6	18.5597	10	15.5936	12	38.4343	40
Papagayos group	*Co. del Medio*	127311	0.512810	4	0.703721	4	18.5970	11	15.6038	13	38.4977	42
		Duplicate	0.512827	3								
	Co. Los Leones SE lava	127424	0.512804	4	0.703845	4	18.5395	12	15.5874	14	38.4186	46
	Top of Co. Guadaloso	127310	0.512795	4	0.703895	6	18.5852	14	15.5941	15	38.4818	46
Rodeo group	*Co. Rodeo*	126078	0.512743	13	0.704158	4	18.5136	11	15.5958	13	38.4240	42
	Co. 1784	126077	0.512820	3	0.703919	4	18.5787	10	15.6080	12	38.5123	40
	Co. Chilena	127327	0.512710	6	0.704116	4	18.5919	17	15.6109	21	38.5221	68
		duplicate	0.512751	4			18.5797	36	15.6092	45	38.5162	149
Diamante group	Co. Diamante, summit	123964[3]	0.512740	5	0.704150	7	18.5070	15	15.6010	20	38.4370	70
	Las Bolas	127437	0.512742	4	0.704106	4	18.5413	14	15.6000	17	38.4395	56
	Co. Negro de las Salinas	127001	0.512784	2	0.703900	6	18.5476	20	15.5989	25	38.4274	81
Loma del Medio	Loma del Medio lava	126083	0.512748	3	0.704182	5	18.5600	15	15.6043	19	38.4850	61
La Leña	*Co. La Leña*	126085	0.512759	4	0.704161	4	18.5624	11	15.5988	13	38.4662	42
Los Reyunos group	*Agua del Toro*	123965[3]	0.512751	4	0.704126	4	18.5080	15	15.5850	15	38.3790	50
	Dique Galileo Vitale	127307	0.512724	5	0.704162	5	18.4843	14	15.6023	17	38.3807	56

1 — Within run error: 1 standard deviation of the mean (SEM), 2 — Within run error calculated by error propagation of errors (SEM) on IC and DS mix runs, 3 — From Søager et al. (2015a, 2015b).

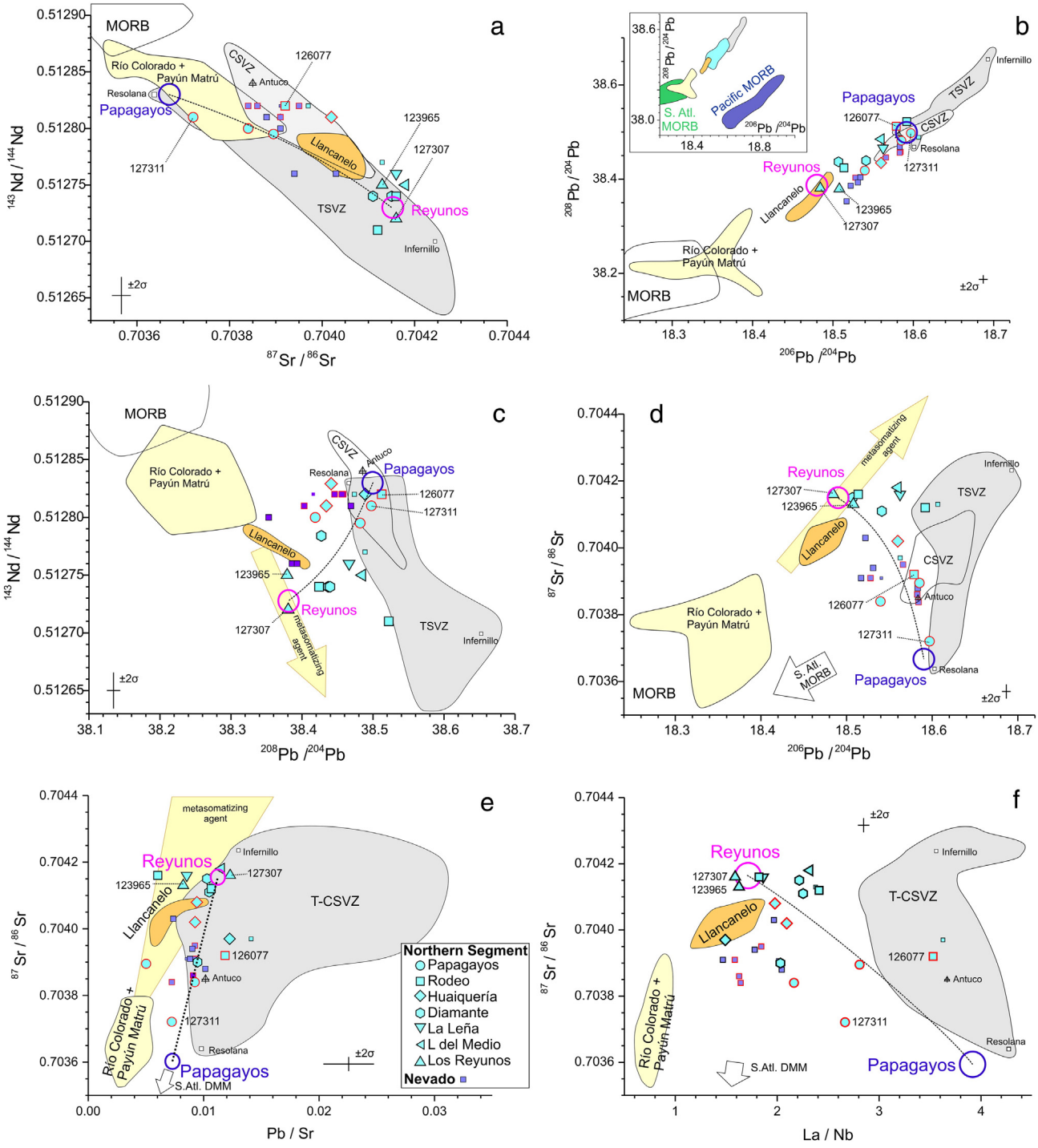

Fig. 3. Radiogenic isotopes for Northern Segment and Nevado. a) $^{143}Nd/^{144}Nd$ vs. $^{87}Sr/^{86}Sr$, b) $^{208}Pb/^{204}Pb$ vs. $^{206}Pb/^{204}Pb$, c) $^{143}Nd/^{144}Nd$ vs. $^{208}Pb/^{204}Pb$, d) $^{87}Sr/^{86}Sr$ vs. $^{206}Pb/^{204}Pb$, e) $^{87}Sr/^{86}Sr$ vs. Pb/Sr, f) $^{87}Sr/^{86}Sr$ vs. La/Nb. Symbols as in Fig. 2, except for triangle with +: Antuco (CSVZ)(CL071), white squares: Resolana (TSVZ) (CL741) and Infernillo (123976), large circles: Papagayos (blue) and Reyunos (magenta) mantle end-members (with tentative mixing curves) — as discussed in text. 4σ error bars for element ratios refer to typical values. (For interpretation of the references to colour in this figure legend, the reader is referred to the web version of this article.)
Data sources: This paper; Jacques et al. (2013); Holm et al. (2014); Søager et al. (2013, 2015a); Søager and Holm (2013); see Supplementary data F for MORB data sources.

Ba, a disadvantage is that trace element ratios are significantly fractionated during mantle melting. For the SVZ arc volcanoes, Holm et al. (2014) found that some arc magmas of the CSVZ (e.g. Antuco) with relatively high Ba/Th were derived from a mantle source metasomatized dominantly by a fluid agent, whereas northwards in the SVZ, an increasing source enrichment was primarily caused by melts derived from UCC-type material with relatively low Ba/Th probably carried down the subduction channel by means of subduction erosion. Subduction erosion at the western margin of South America has been proposed by several workers (e.g. Kay et al., 2005; Stern, 1991). Using this model, and assuming other things being equal, the relatively low Ba/Th of the Northern Segment rocks relative to the Antuco source (Fig. 5a and c) also requires a UCC component in their source. This is also indicated when comparing to results of fluid experiments (Brenan et al., 1995; Kessel et al., 2005) in Fig. 5a (red lines). Vice versa, it is evident that some fluid enrichment of the source is required for the Northern

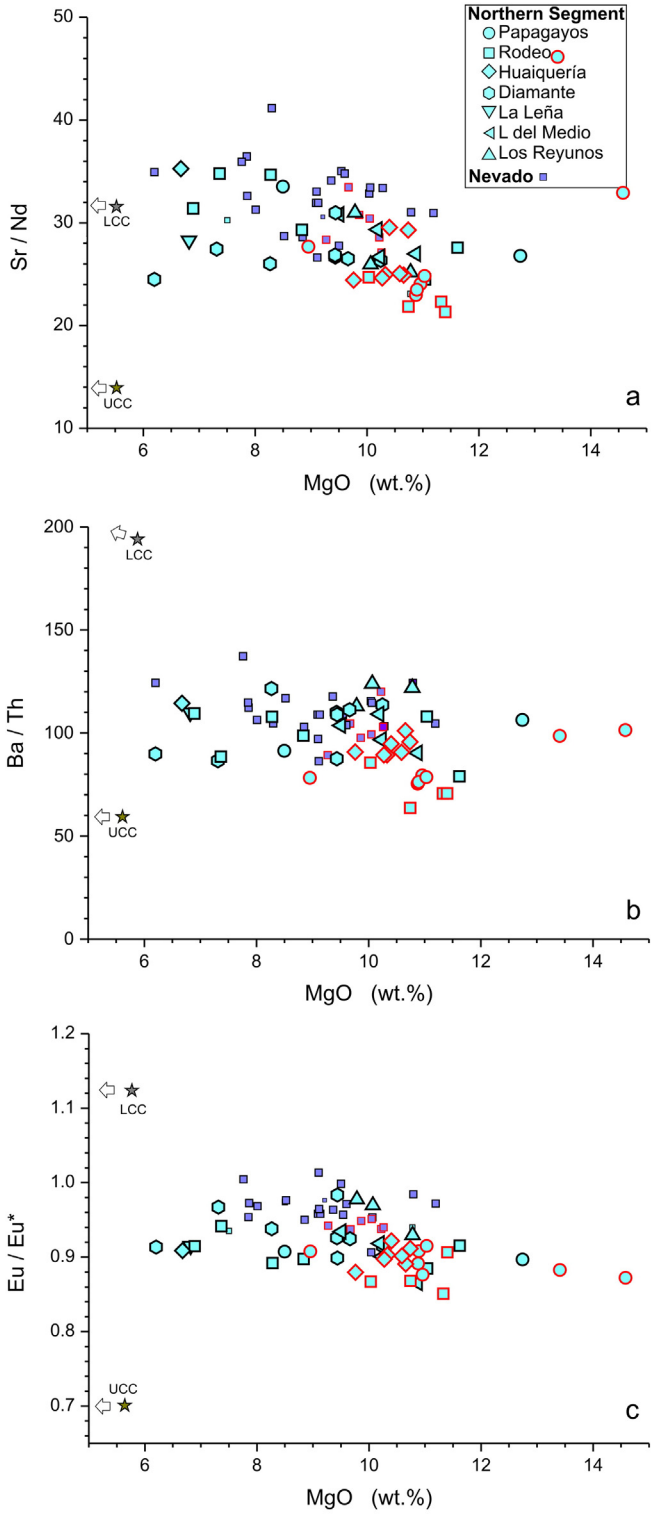

Fig. 4. a) Sr/Nd, b) Ba/Th and c) Eu/Eu* vs. MgO for the Northern Segment volcanic rocks. Average upper (UCC) and lower (LCC) continental crust (Rudnick and Gao, 2003) are shown for comparison. The lack of correlation counterindicates any overall importance of afc-type processes in the analysed Northern Segment magmas.

Segment rocks, because a mantle source enriched solely with e.g. average UCC (Rudnick and Gao, 2003) will not be able to produce the Ba/Th ratios of the backarc or arc rocks, since partial melts of such a mantle will plot on the mixing trajectory of the pre-enrichment mantle and UCC (green lines in Fig. 5a). Some of these alkaline basalts have high Ba/Sm and Th/Sm compared to most TSVZ arc rocks at comparable Ba/Th. This is probably due to their derivation by slightly lower degrees of mantle melting (3–7% in Fig. 5a) relative to the calc-alkaline basaltic andesites of the TSVZ arc, which were argued to be derived by 5–10% melting by Søager et al. (2015a). The variation of the studied samples conforms to trends generated by variable melting (blue lines in Fig. 5a) at near constant Ba/Th for most samples (Fig. 5a).

Reduction in fluid-borne addition to the mantle (with or without a UCC-component) would alone cause the Ba/Th in the mantle and its melts to be reduced. To test this alternative, the compositional variation of Nb/Th is considered. The pre-metasomatic mantle (of e.g. PM to DDMM composition) has a much higher Nb/Th ratio than melts from the C-T-NSVZ as well as Northern Segment rocks, which are indicated to have a significant UCC component. With decreasing Ba/Th also Nb/Th decreases for these rock groups, and Th increases in accordance with an increasing upper crustal component supplying the Th-enrichment. A reduced enrichment of an Antuco-type CSVZ source in fluids has mainly influence on Ba in Ba-Th-Nb space, and would not generate the observed three-fold increase in Th, and is thus ruled out.

Mantle melting strongly fractionates La/Sm and Nb/Sm ratios (Fig. 5b) but not La/Nb. Søager et al. (2015a) showed that residual rutile had none or very small influence on Nb in Nevado magmas. The 6-fold variation of La/Nb in Payenia magmas, therefore, most likely reflects source compositions. The OIB-type magmas of Río Colorado and Payún Matrú require melting of primordial mantle (PM) or even more Nb-enriched mantle with higher Nb/Sm than PM and La/Nb < 1 (Fig. 5b). By contrast, all other arc and backarc magmas need sources enriched relatively in La. From the modelling illustrated in Fig. 5b it is clear, that the pre-metasomatic source of the volcanic arc magmas must have been more depleted than the depleted MORB mantle (DMM) of Salters and Stracke (2004) because CSVZ magmas have Nb/Sm ranging lower than DMM. Their source could be similar to Depleted DMM (Workman and Hart, 2005) as also suggested by Søager et al. (2015a). We therefore need to modify the DMM model of Holm et al. (2014) for the Antuco source, which instead needs a more depleted source, such as Depleted DMM (Fig. 5b). An equally depleted pre-metasomatic source is required for some Rodeo and Papagayos magmas of the Northern Segment.

Quantitative modelling of melting assumed a peridotitic source and was by pooled incremental non-modal batch melting of peridotite (for details see Supplementary data E). For example, some Rodeo samples (e.g. 126077) can be modelled (Fig. 5a) as derived by around 5% melting of a Depleted DMM type mantle enriched by 2% UCC' and a fluid addition of Ba (increasing Ba/Sm to 65) (Fig. 5a). This model for 126077 also applies for Nb–La–Sm (Fig. 5b). Although relative effects of contributions from UCC and fluids can thus be modelled, the amount of fluid involved remains unconstrained. UCC' is the modification of the average UCC of Rudnick and Gao (2003) by increasing Th and U and reducing Sr and Eu to suit modelling of arc magmas by Holm et al. (2014). As an approximation in our modelling, we assume no addition of Th via the fluid enrichment (Fig. 5a).

The Northern Segment magmas with higher Nb/Sm than arc magmas must have had a pre-metasomatic source which was less depleted than arc magma sources (Fig. 5b). For the Northern Segment rocks with the lowest La/Nb of 1.5, i.e. 127307 at Galileo Vitale (and most Nevado basalts), the maximum UCC enrichment of a PM source based on its Th/Sm = 0.42 is c. 1% UCC' (Fig. 5a), and it is clear that the pre-metasomatic source must have been more enriched than DMM to get comparable degrees of melting (c. 6%) in Fig. 4a and b. We model these low La/Nb rocks with a PM source, as Søager et al. (2015a) also used to model the Nevado basalts. We therefore see an overall increase in pre-metasomatic mantle source enrichment represented by increasing Nb/Sm in the backarc basalts from north to south (Fig. 6a).

High Sr/Nd in rocks with no Eu-anomaly, such as Antuco (Sr/Nd = 36, compared to Sr/Nd = 13–16 in various mantle rocks, Fig. 5d),

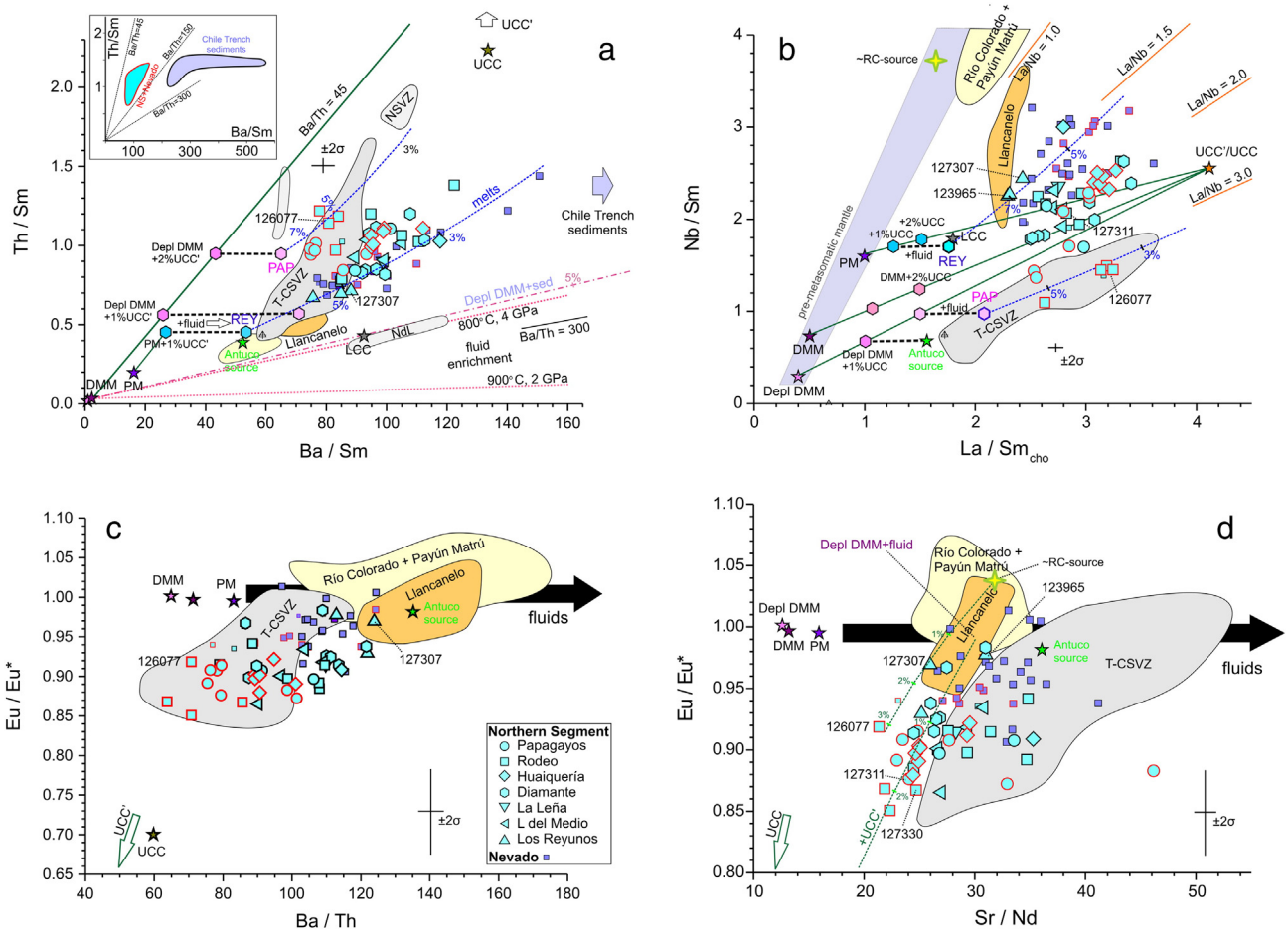

Fig. 5. Trace element modelling of Northern Segment and Nevado magmas. a) Th/Sm vs. Ba/Sm, b) Nb/Sm vs. La/Sm, c) Eu/Eu* vs. Ba/Th, d) Eu/Eu* vs Sr/Nd. Symbols as in Fig. 2, and PM = Primordial Mantle, DMM = Depleted MORB Mantle, Depl DMM = Depleted DMM, UCC = average upper continental crust, UCC' = modified average UCC, LCC = average lower continental crust. See text for discussion of choice of incompatible elements and for mantle sources, crustal compositions and melting. Fluid enrichment model in a): dotted red lines: enrichment of fluid derived from DMM at 4 GPa (Kessel et al., 2005), and at 2 GPa (Brenan et al., 1995). Chile Trench sediments: Jacques et al. (2013) and Lucassen et al. (2010), and red dot-stipple line is mixing between DMM and sediment SO210–#05_B. NdL — high Ba samples of Nevado de Longaví volcano in the CSVZ. In a–d: Bold fat stiples: enrichment of mantle with fluids, Green lines: mixing of mantle and UCC'. Blue stipple: melting curves with tick marks for degree of melting. Black arrow in c–d: enrichment by fluids derived from mantle source without Eu-anomaly. In d green dashed curves show the effect of addition of UCC to two mantle compositions: fluid-enriched Depleted DMM and RC (Río Colorado) OIB-type, respectively. In a–b: PAP — Papagayos and REY — Reyunos end-members as discussed in text. 4σ error bars refer to typical values. (For interpretation of the references to colour in this figure legend, the reader is referred to the web version of this article.)
Data sources: PM (Sun and McDonough, 1989), DMM (Salters and Stracke, 2004), Depleted DMM (Workman and Hart, 2005), UCC (Rudnick and Gao, 2003), Antuco source and UCC' (Holm et al., 2014), other Payenia rocks: as in Fig. 2.

indicates source enrichment by fluids and a low UCC input (Holm et al., 2014), whereas Eu/Eu* = 0.85 to 0.95 and Sr/Nd down to 22 for most Northern Segment rocks require 0.5–3% UCC' in addition to the fluid input in our modelling. The amount will in each case depend on the REE abundances of the pre-metasomatic mantle and crustal melt. The variation of Eu/Eu* is clearly outside the analytical error (Fig. 5c and d), and the good correlation ($r^2 = 0.94$) of Eu/Eu* calculated from Sm–Gd and Sm–Tb, respectively, shows that the Eu-anomaly is not an artefact of a high Gd/Sm component. The positive correlation of Eu/Eu* with both Ba/Th and Sr/Nd (Fig. 5c and d) further testifies that upper continental crust is involved. It is further evident that the negative Eu anomaly and thus the UCC component of the magmas increases northward in Payenia (Fig. 6b). However, some Northern Segment rocks with relatively high Ba/Th and Nb/Sm (e.g. 127307) have very small negative Eu-anomalies, and the source for these can be modelled predominantly by a fluid enrichment. UCC components <0.5% cannot be ascertained because identification of a negative Eu-anomaly requires this addition to change Eu/Eu* outside the (2σ) analytical error. Alternatively, a UCC component may be accommodated if the pre-metasomatic source had a positive Eu-anomaly and relatively high Nb/Sm, Ba/Th and Sr/Nd as seen in the OIB-type Río Colorado magmas.

5.2. Mantle enrichment by sediments versus subduction eroded crust

Subducted sediment has been suggested to be an important component in many arc magmas (e.g. Plank and Langmuir, 1993; Tatsumi and Kogiso, 2003). If sediment-derived, the upper crustal component in Payenia backarc magmas could be expected to be sediments similar to those of the present day Chile Trench. Dredged Chile Trench sediments at 33–36°S along TSVZ have high Ba/Sm = 246–559 and Ba/Th = 176–384, whereas further south, along the CSVZ at 36–39°S, they have lower Ba/Sm = 80–191 and Ba/Th = 68–143 (Jacques et al., 2013; Lucassen et al., 2010). By contrast, Ba/Th decreases northwards in the SVZ arc rocks, and both TSVZ arc and backarc rocks have much lower Ba/Th than the sediments north of 36°S (Fig. 6c). High concentration in the sediments of incompatible elements, such as Ba, would be a feature transferred into sediment melts and thus to the mantle enriched by such melts. These contrasts between compositions and trends of sediments and magmas are strong indications against an important

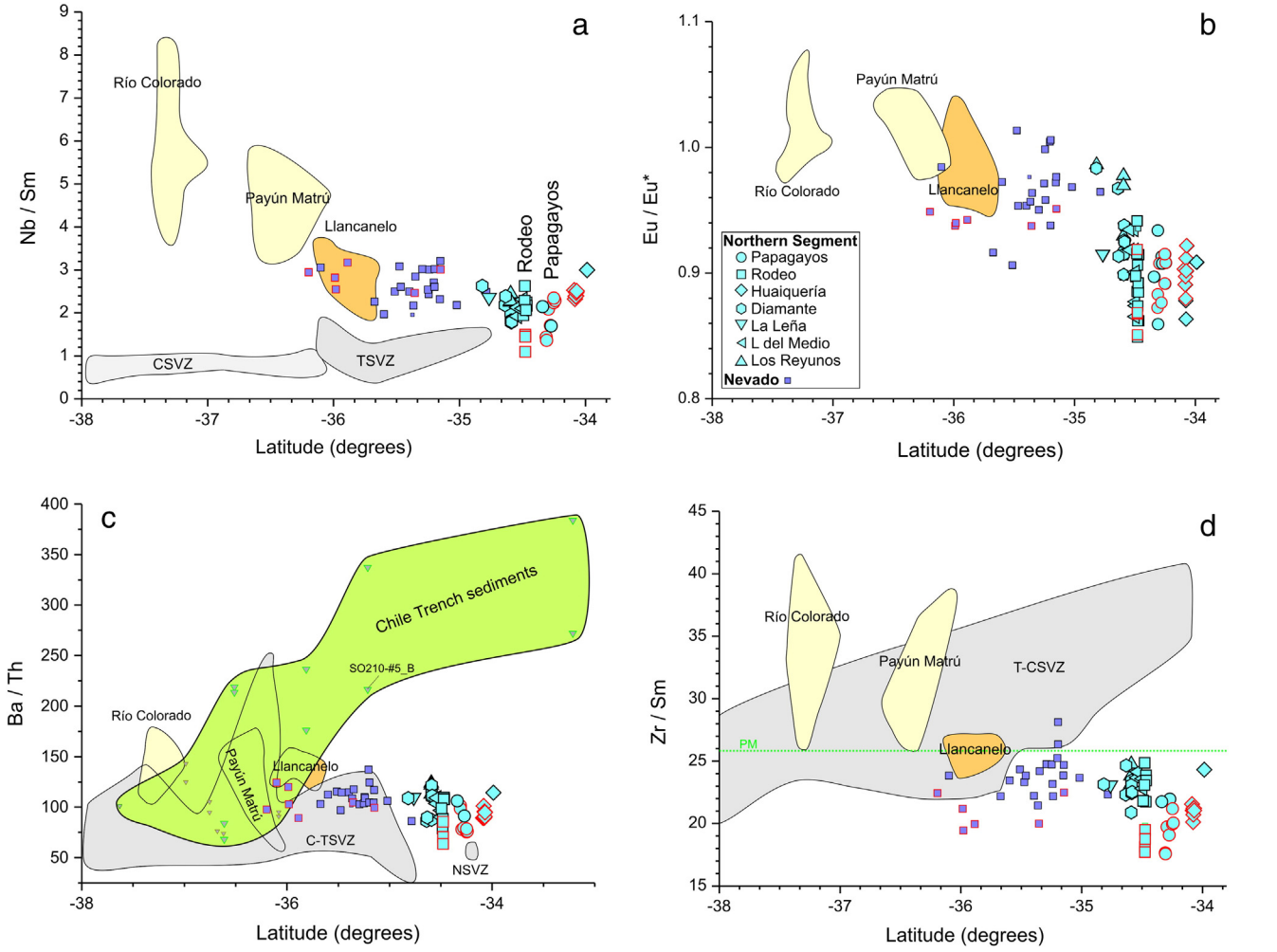

Fig. 6. Trace element ratio variations with latitude: a) Nb/Sm, b) Eu/Eu*, c) Ba/Th and d) Zr/Sm. There is a northwards increasing mantle component of UCC in Payenia illustrated by decreasing Eu/Eu*, and this component has low Zr/Sm, whereas high Nb/Sm in southern Payenia indicates less depleted pre-metasomatic mantle sources. Chile Trench sediments (Lucassen et al., 2010; Jacques et al., 2013) at 33–35.5°S have much higher Ba/Th than arc and backarc rocks.

sediment contribution to mantle source enrichment in the TSVZ arc and backarc. Model addition of sediment (Chile Trench at 35°S sample SO210-#05_B of Jacques et al., 2013) to PM or DM results in source compositions with Ba/Th as high as in fluids, and cannot explain the Northern Segment or Nevado (or SVZ) samples (Fig. 5a). Also, the correlation of Nd and Sr isotopes of the sediments cannot be reconciled with their significant incorporation into the mantle source of the T-NSVZ arc, as discussed in detail by Holm et al. (2014), and the same arguments apply to the backarc. It is thus highly unlikely that the trench sediments are important contributors to the arc or backarc magmas. Instead, we suggest that melts of subduction eroded crust enriched the backarc mantle source of the Northern Segment and Nevado Volcanic Field magmas.

Our modelling for the Northern Segment and Nevado, therefore, suggests that pre-metasomatic sources ranging from highly depleted to undepleted mantle were enriched by c. 1–2% UCC', and by fluids. For the Northern Segment, the compositional differences to the arc magmas are probably to some extent caused by slightly lower degrees of melting (i.e. 3–8%), but in particular they reflect the strong variation in degree of depletion of the pre-metasomatic sources, which are in most cases less depleted than beneath the arc. The Northern Segment and other Payenia rocks thus indicate that the enrichment of the pre-metasomatic sources in general increases southwards in the backarc (Fig. 6a). However, we note that the Northern Segment source variation must also be present on a rather small scale, because at both Rodeo and Papagayos much of the total Northern Segment source compositional range is displayed by magmas erupted only a few km apart. Also, it is worth noticing, that there is no indication of a temporal change in the geochemistry of the magmas of the Northern Segment.

5.3. Low Zr/Sm source ratios

Many Northern Segment and Nevado backarc rocks have lower Zr/Sm than PM (26), MORB and the OIB-type rocks of Río Colorado and Payún Matrú, and all Northern Segment rocks have lower Hf/Sm than PM (0.70) (Fig. 7a, e–f). Zr/Sm ranges to a low of 17 in those rocks of Rodeo and Papagayos having the most depleted pre-metasomatic sources, and the low relative abundances of Zr and Hf are also apparent as a Zr–Hf trough in the incompatible element patterns (Fig. 2f). Much of the variation of Zr/Sm found in many arcs seems to be caused by the increase of this ratio during fractional crystallization, mainly as a result of clinopyroxene and amphibole having $D_{Zr/Sm} < 1$ (Handley et al., 2011; Thirlwall et al., 1994). This cannot be the cause of the variation in the primitive Northern Segment and Nevado rocks, which fractionated only olivine, and, as pointed out by Handley et al. (2011), because clinopyroxene $D_{Zr/Sm}$ seems to approach 1 in silica-poor rocks. Moreover, the Northern Segment and Nevado rocks display no correlation of Zr/Sm with Mg# (not shown). Chauvel and Blichert-Toft (2001) and Pearce et al. (1999) found that during mantle melting and early stages of magmatic fractionation only a little fractionation of Hf/Sm

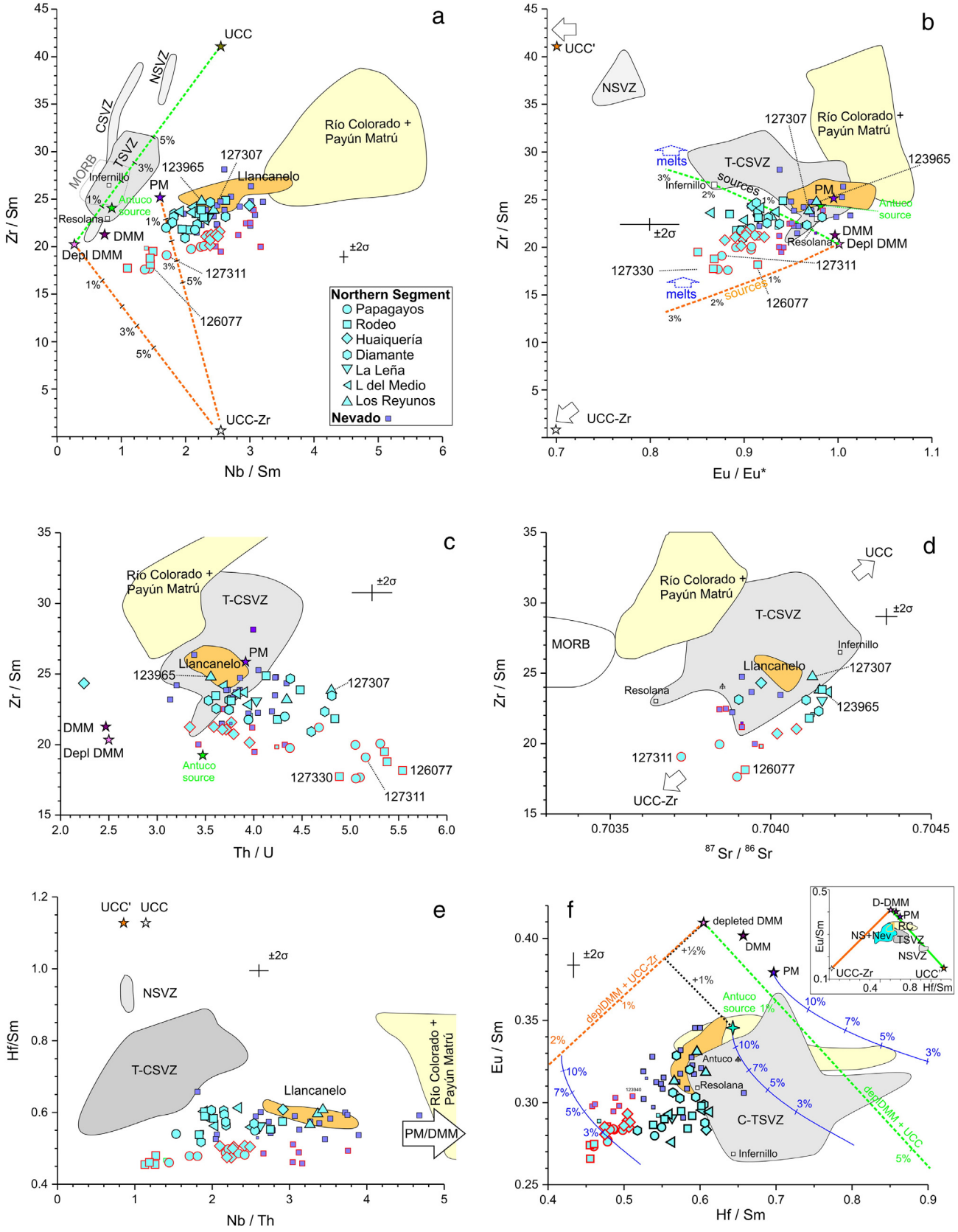

Fig. 7. a) Zr/Sm vs. Nb/Sm, b) Zr/Sm vs. Eu/Eu*, c) Zr/Sm vs. Th/U, d) Zr/Sm vs. $^{87}Sr/^{86}Sr$, e) Hf/Sm vs. Nb/Th, and f) Eu/Sm vs. Hf/Sm. Symbols as in Fig. 2 and abbreviations as in Fig. 5. Green stipple: mantle + UCC', orange stipple: mantle + UCC-Zr, tick marks: % UCC added. Blue arrows in b indicate that melts have higher Zr/Sm than the mantle sources. Blue lines in f: melting curves. 4σ error bars for element ratios refer to typical values. (For interpretation of the references to colour in this figure legend, the reader is referred to the web version of this article.)

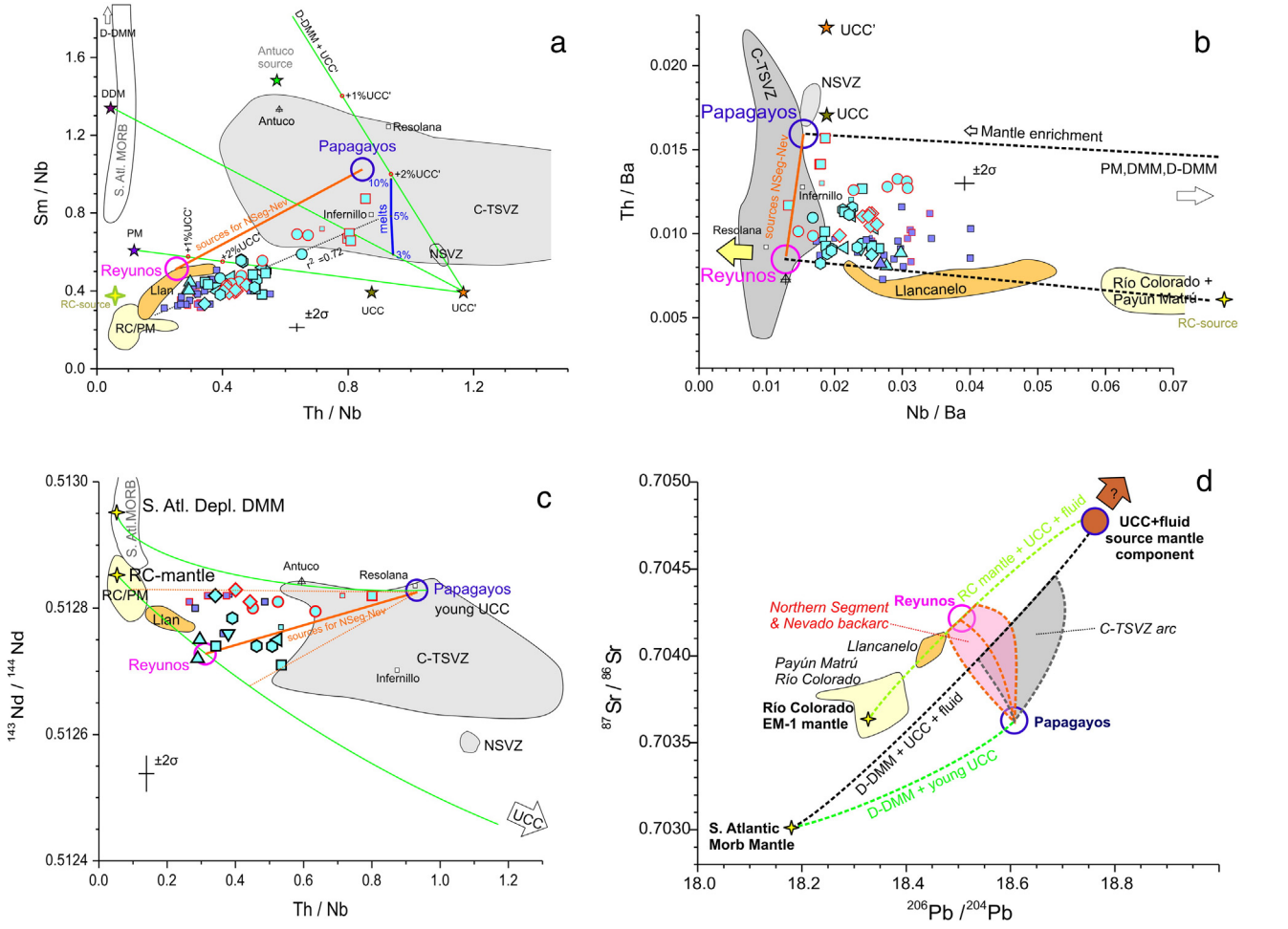

Fig. 8. a) Sm/Nb vs. Th/Nb, b) Th/Ba vs. Nb/Ba, c) $^{143}Nd/^{144}Nd$ vs. Th/Nb. Modelled compositions of enriching agents added to the pre-metasomatic mantle of the end-members Papagayos and Reyunos. All Northern Segment and Nevado rock can be derived by around 5% melting of mixtures of Papagayos and Reyunos mantle. In this diagram highly fluid soluble elements are not represented. Reyunos mantle is one of mantle compositions generated by enrichment of RC mantle, which is characterized by low Th/Ba, characterized by a relatively high importance of fluid soluble elements resulting in its low Th/Ba ratio. Papagayos mantle with its relatively high Th/Ba is indicated to have been enriched relatively more by a UCC component. Papagayos mantle is argued to be young (perhaps Mesozoic) and have approximately the Nd isotopic composition of its UCC component, whereas the UCC component of Reyunos mantle may have significantly more unradiogenic Nd. Symbols as in Fig. 2. Yellow stars: representative compositions for Río Colorado (RC) and South Atlantic Depleted MORB mantle (see text for discussion). Blue circle — Papagayos mantle composed of Depleted DMM plus 1–2% UCC' (in this diagram UCC' identical to UCC-Zr), Magenta circle — Reyunos mantle composed of approximately PM (resembling RC mantle) plus UCC'. 4σ error bars for element ratios refer to typical values. (For interpretation of the references to colour in this figure legend, the reader is referred to the web version of this article.)

occurs, whereas Frey et al. (2015) note that $D_{Hf/Zr}$(cpx/melt) ~ 2 for mantle rocks. However, the most Zr-depleted rocks have Zr/Hf = 36–38, and these elements are thus unfractionated relative to PM or depleted mantle values of 34–40. The low Zr/Sm and Hf/Sm in the backarc therefore seem to be largely inherited from the mantle source, and we have marked the symbols of these rocks (with Hf/Sm < 0.52) with a red outline in all figures.

Most TSVZ arc rocks have higher Zr/Sm (up to 32) and Hf/Sm than the backarc. Together with mafic Maipo rocks of the NSVZ with high Zr/Sm = 35–40, primitive TSVZ rocks trend from Antuco with Zr/Sm = 24 towards UCC in accordance with the model of Holm et al. (2014) of a northward increasing UCC component in the source (Fig. 7a). Because of the separation of the arc and backarc magmas in Fig. 7a and b the UCC components in the two must be different. The backarc rocks with the strongest UCC signature, i.e. highest Th/Sm, La/Nb, and Th/Ba, and lowest Eu/Eu*, have the lowest Zr/Sm and low Hf/Sm = 0.45–0.48. These rocks also tend to have higher Th/U = 4.5–5.5 than the arc rocks and also higher than other backarc rocks, which mostly have values of 3.1–4.4 (Fig. 7c). This suggests that Th/U, Zr/Sm, and Hf/Sm ratios were fractionated by the same process, and that this process encompasses the addition of a UCC component to the mantle source. The difference between the crustal melts suggested to have metasomatized the mantle beneath the arc and backarc, respectively, could be that zircon was residual in the melting of the subducted crust under the backarc, but not under the present day arc. Residual zircon will retain Zr (and Hf) and fractionate Th/U because the compatibilities of these two latter elements are very different. Similarly, low Hf/Sm in basaltic arc rocks from Java was proposed to be a feature of their mantle source, which was, however, enriched by melts of sediment with residual zircon (Handley et al., 2011), and negative Hf and Zr anomalies in subduction zone magmas were suggested to be caused by residual zircon in subducted sediments by Hermann (2003).

We modelled melting of crust with residual zircon and added the melts (called UCC-Zr) to mantle rock based on the modelling above (Fig. 7a and b, for details see Supplementary data E). A large degree of melting (F = 0.8) ensured almost identical incompatible element ratios in crust and melt, and the feasibility to have residual zircon in high degree melts of sediments at subarc pressures and temperatures has been demonstrated by Hermann and Rubatto (2009). The lack of correlation of Zr/Hf with Zr/Sm and Hf/Sm (not shown) is expected, if D(zircon/melt) for Zr and Hf are rather similar and very high, as found by e.g. Rubatto and Hermann (2007). However, samples with low Hf/Sm

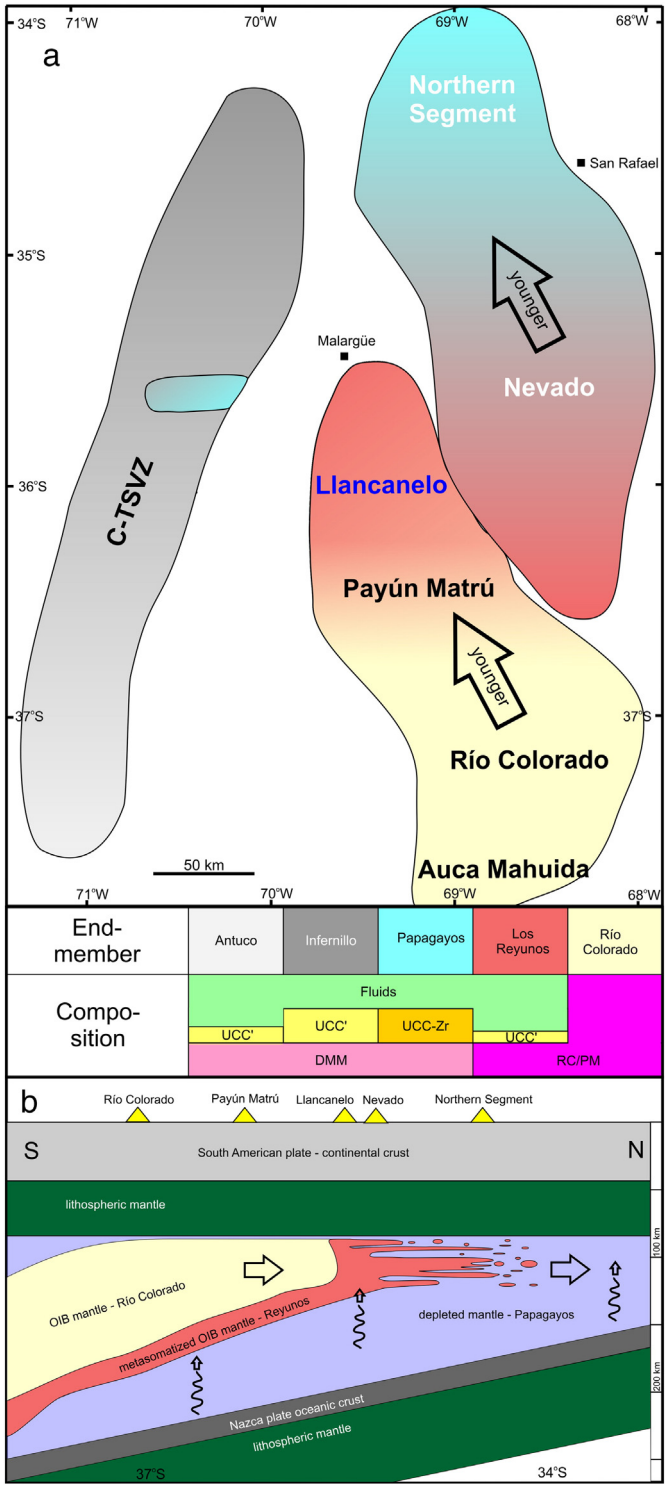

Fig. 9. Model for the lateral relations between identified mantle compositions in the backarc and arc. For each volcanic field in the backarc and subzone of the SVZ it is indicated which end-members are mixing. The legend shows mantle end-members and their compositions. The southwards fading of the Reyunos mantle contribution to the southern Payenia magmas reflects the decreasing fluid/UCC contribution to the upwelling mantle. The southward increase in depth to the Nazca plate is mainly due to increasing horizontal distance to the trench for a S–N section (see Fig. 1).

among Nevado rocks with the highest Nb/Sm and Nb/Th (Fig. 7a and e) show that this UCC component was present in places throughout this part of the backarc.

We have also quantified the effects of addition of UCC with and without residual zircon to the pre-metasomatic mantle. Both UCC components have strongly negative Eu-anomalies but contrasting Hf/Sm ratios. During spinel peridotite melting Hf, Eu, and Sm have only slightly different partitioning coefficients, e.g. we use those of Hill et al. (2011) for clinopyroxene (see also Supplementary data E), and melting trajectories in Eu/Sm vs. Hf/Sm (Fig. 7f) are semi-parallel to mixtures of pre-metasomatic mantle and average UCC (Rudnick and Gao, 2003). Therefore the effect of addition of UCC melts with residual zircon (UCC-Zr) is identifiable (Fig. 7f). The Papagayos source is indicated to have up around 2% UCC-Zr added to depleted DMM. A somewhat surprising indication in Fig. 7f is that most arc and backarc magmas had sources with some UCC-Zr component. The Antuco (CSVZ) source in this scheme requires 1/2% of UCC-Zr plus 1% UCC', and for other C-TSVZ even more UCC-Zr is required (Fig. 7f). However, use of different literature partitioning coefficients leads to considerable variation in calculated proportions.

Residual rutile during melting can deplete the melts in Nb, Ta, Zr, and Hf, and is expected to increase Nb/Ta and Zr/Hf in the melts (Klemme et al., 2005). However, in the Northern Segment rocks, Zr/Sm and Nb/Sm are not correlated with Nb/Ta or Zr/Hf, and Nb/Ta and Zr/Hf are within the same range as the southern Payenia OIB-type basalts. Neither of these ratios thus indicates significant residual rutile in the source for Northern Segment rocks. In addition, no or only minor rutile was concluded to have been present in the Nevado mantle sources (Søager et al., 2015a). Effects of other potential residual accessory minerals are also missing. Residual allanite would lower Th/U in the magmas (Ewart and Griffin, 1994), residual monazite or apatite would result in low contents of e.g. REEs, Th and U (e.g Stepanov et al., 2012) and thus would not cause the observed low Zr–Hf/REE and high Th/U ratios.

5.4. Mantle end-members and the relationship with OIB-type and arc magmas

Sr–Nd–Pb isotopes of the SVZ arc at the latitudes of Payenia define an array unaligned to the array of OIB-type magmas of Río Colorado, Payún Matrú and Llancanelo (Fig. 3c–d), although the incompatible element enrichment of the latter is transitional between OIB and subduction zone type (Espanon et al., 2014a; Søager et al., 2013, 2015a). The alkaline Northern Segment and Nevado rocks define an array which trends obliquely to the trends of the two other arrays. One end-member of the trend is represented by the Reyunos group (average of Galileo Vitale 127307 and Agua del Toro 123965 with high Nb/Sm, Fig. 5b, and Nb/Th, Fig. 7e), which isotopically is not very different from the end of the Llancanelo compositional field. The other end-member is defined by samples from Papagayos (127311) and Rodeo (126077) (their average) with low Nb/Sm and Nb/Th, the Papagayos end-member, and overlap with TSVZ samples from Resolana of the Co. Azul volcano. The Papagayos mantle end-member has rather unradiogenic Sr and radiogenic Nd, but has a strong subduction zone type enrichment (Figs. 3 and 2f).

The Northern Segment and Nevado magmas cannot all be explained by melting after mixing of the two end-members, Papagayos and Reyunos. The range of possible mixing trends to explain the samples indicates varying Sr/Nd, Pb/Nd and Sr/Pb ratios in Reyunos and Papagayos mantle rocks (Fig. 3a and c–e). However, mixing curves to explain all samples would require considerable variation in the ratio $(Sr/Nd_{Reyunos})/(Sr/Nd_{Papagayos})$ from near unity (0.7 for model end-members) to values $\gg 1$, and the same applies to Pb/Nd. Alternatively, Reyunos is a variable component that can be considered part of an array extending from the Río Colorado end-member, over Payún Matrú and Llancanelo, to a composition defined by a fluid-borne enrichment plus a less important UCC melt. These compositions could have been formed by variable metasomatism of Río Colorado OIB-type mantle by the fluids/UCC melts. This would allow all Northern Segment plus Nevado samples to be explained by mixing of the relatively well constrained Papagayos mantle end-member with Río Colorado mantle

plus a variable fluid/UCC melt component as indicated by an arrow in Fig. 3c–e. This is discussed further below.

The Papagayos end-member had a depleted pre-metasomatic mantle source enriched by UCC-Zr melts (with low Eu/Eu* and high Th/U), and the fluid component in the derived magmas was relatively small (resulting in low Sr/Nd and Ba/Th in the end-member), and it is thus also geochemically distinct from the Reyunos component. Papagayos is moreover an end-member for at least some TSVZ arc magmas. Therefore, the compositional variation in the SVZ from the CSVZ (Antuco end-member of mainly fluid-enriched depleted mantle) to Infernillo (the volcanic complex in TSVZ with the most radiogenic Sr and Pb, and least radiogenic Nd derived from depleted mantle enriched dominantly by UCC') (Holm et al., 2014) also encompasses a third component, the Papagayos end-member (most strongly present in the samples from the Resolana volcano), which has the lowest $^{87}Sr/^{86}Sr$ in the TSVZ (Fig. 3).

5.5. Further constraints on the mantle source components

The abundances of Nb, Th, and Sm in the magmas are relatively insensitive to the component added to the mantle sources by fluids, and we use these elements to further constrain the enrichment by UCC of the Papagayos and Reyunos mantle (Fig. 8a). Pre-metasomatic mantle compositions have relatively low Th/Nb but highly variable Sm/Nb. UCC' enrichment by 1–2% of Depleted DMM will model the Papagayos source necessary to explain many Northern Segment magmas. The Reyunos source needs a similar degree of UCC' enrichment of a Río Colorado type source. Nevado and Northern Segment magmas can be modelled by melting of mixtures of Papagayos and Reyunos mantle sources. The rocks trend parallel to the suggested source mixing line in Fig. 8a as expected for the magmas. We note that C-TSVZ magmas are indicated to be derived from depleted mantle with notable UCC components, some of which are required to have higher Th/Nb than the UCC' used for our modelling of the backarc magmas. This is instead likely an effect of some solubility of Th in fluids contrary to our initial assumption of insolubility used as an approximation.

All rocks of the Northern Segment and Nevado have low ratios of Nb/Ba (<0.04) compared to mantle compositions such as PM, DMM, and Depleted DMM (0.10–0.32) (Fig. 8b). We have argued that high Th/Ba is caused by a UCC component, whereas low Th/Ba is caused by a fluid-borne source enrichment, and it is clear from Fig. 8b that Papagayos mantle is dominated by a UCC component, whereas Reyunos mantle had a larger fraction of its enrichment by fluids. The most Ba enriched Northern Segment rocks have compositions overlapping the field for C-TSVZ arc rocks.

The isotopic composition of the enriching agents for the pre-metasomatic mantle sources cannot be precisely defined. Because the Reyunos source was mostly fluid enriched, no specific UCC component is indicated. Sr and Nd isotope variations (Fig. 3a) require the Papagayos enrichment to be by relatively young UCC melts, and these could be related to Late Mesozoic or Tertiary intrusive rocks (Lucassen et al., 2004).

Our proposed model for the relationship between the components is illustrated in Fig. 8d (see also Fig. 3d). The Reyunos mantle is envisaged as generated by variable addition of fluids and UCC melt to the pre-metasomatic Río Colorado-type mantle, as it is also the case for the mantle source of the Llancanelo magmas. To generate most of the Northern Segment and Nevado magmas, the Reyunos mantle was accompanied by variable amounts of Papagayos mantle, which is modelled as South Atlantic depleted mantle plus melts of young UCC melt and a limited fluid component. The arc magmas of the C-TSVZ can be derived by three components. The well-defined composition of the Papagayos component (Fig. 8) may be speculated to indicate that it was added to the source after the other components mixed.

The Northern Segment and Nevado magmas seem to be derived from mixtures of originally depleted (Papagayos) and undepleted (Reyunos) mantle, both enriched over the subduction zone. A sketch of our model for the relationship between the Payenia mantle domains and their relative contributions to the magmas are shown in Fig. 9. The Llancanelo rocks show that Reyunos mantle also interacts with, or have a component of, the Río Colorado OIB-type mantle. Therefore, the subduction zone enriched Llancanelo/Reyunos mantle is likely a part of the body of OIB-type mantle upwelling beneath the southern part of the backarc (Burd et al., 2014; Søager et al., 2015b) and received its subduction zone enrichment from the subducting slab when entering the mantle wedge. The Río Colorado basalts are thought to have been derived primarily by melting of pyroxenite present in a peridotite matrix (Søager and Holm, 2013; Søager et al., 2015b). Fluid fluxing metasomatized and lowered the solidus of the peridotite of this composite mantle, and caused this originally less enriched mantle to produce the Reyunos type magmas.

To the east and north in the backarc Papagayos mantle mixed variably with Reyunos mantle, resulting in an overall decrease in the Reyunos component northwards. There does not seem to be any component of Río Colorado-Reyunos mantle in the arc mantle, whereas Papagayos mantle is most clearly manifest in Resolana but plays a minor, but significant, role in the arc (e.g. Fig. 7a and f).

In the arc the main isotopic variation is defined by UCC and South Atlantic MORB mantle with no clear contribution from the slab (Holm et al., 2014; Jacques et al., 2013). In the Northern Segment and Nevado backarc two distinctly different subduction zone components dominate the isotopic variation of the magmas. One is the low Zr/Sm UCC-Zr melts of the Papagayos end-member. The other is the fluid-dominated component of the Reyunos end-member.

5.6. The origin of the solutes of hydrous fluids in the backarc and arc of the SVZ

Hydrous fluids have been shown to play an important role in the generation of the incompatible element budget of backarc magmas of Northern Segment and Nevado. In our modelling for sample 126077 (Fig. 5) the contribution of Ba from a fluid is around half of that from UCC, and for La it is around a third, and the Papagayos mantle is not very different in this respect. If the fluids originated in the Nazca plate it may therefore appear surprising that slab-derived fluid mobile elements like Pb and Sr have left little or no signal in the isotopic composition of the Northern Segment magmas, considering, in particular, the distinctly different Pb isotopic compositions of Pacific MORB (Fig. 3b inset). The same is the case for the arc rocks investigated by Holm et al. (2014), and Jacques et al. (2013) proposed a model where fluids were not even required to generate arc and backarc magmas. The trend of Pb isotopes in the backarc as well as the SVZ arc does not allow substantial amounts of Pb derived from Pacific oceanic crust or mantle. On the contrary, the Pb isotopes show that the major components must predominantly be South Atlantic MORB mantle and continental crust or sediments, as already discussed. This suggests that the fluids, which we show are clearly involved, derived their isotopic compositions also from these components. It has been argued that chlorite break-down in the rock assemblage of the subduction channel is the main contributor to hydrous fluids related to arc magma genesis because chlorite is stable to higher P–T conditions than other hydrous minerals, e.g. amphibole or serpentine, hosting water in subducting oceanic crust and mantle at relatively shallow levels (e.g. Grove et al., 2009). However, chlorite carries no significant amount of incompatible elements (El Korh et al., 2009; Marshall and Schumacher, 2012; Scambelluri et al., 2014). Therefore, if the released hydrous fluids do not react with sinks for slab-derived elements in their source, they will instead acquire their enrichment of hydrophile elements, including their isotopic composition, through leaching of the wedge mantle as they rise. As already discussed, we see no significant indication for residual accessory minerals in the geochemistry of the magmas other than zircon in some subducted UCC. Therefore, the fluids may not have isotopic compositions different from the mantle wedge. An origin of the trace

elements in the fluids from the wedge would also explain why even the particularly fluid enriched Nevado de Longaví arc magmas (Fig. 5a) (Rodríguez et al., 2007; Sellés et al., 2004) do not show a variation in $^{87}Sr/^{86}Sr$ correlated with degree of fluid enrichment (e.g. with Ba/Nb). The implication is that the magmas discussed here will have isotopic compositions reflecting the pre-metasomatic mantle plus melts of subducted crustal materials, but not the subducted slab from which the water originally stems. Element concentrations, on the other hand, are influenced by fluid-rock partitioning during fluid percolation. This also explains why the rocks proposed to be mixtures of Papagayos and Reyunos require variable Sr–Nd–Pb element ratios.

5.7. Scenario for mantle development under northern Payenia

The cause for sub-arc melting in the mantle wedge is generally thought to be a lowering of the mantle solidus by addition of a hydrous fluids generating calc-alkaline or tholeiitic magmas (e.g. Gaetani and Grove, 2003; Hirose, 1997). In the case of the alkaline Northern Segment magmas this mechanism seems to be much less predominant than for the frontal arc magmas, and the lower silica and higher alkali contents indicate low P_{H2O} in the mantle source and lower degrees of melting, as also suggested above by the trace element modelling.

In the Plio–Pleistocene, the subducting Nazca plate increased its inclination from shallow in the Late Miocene (Dyhr et al., 2013b; Kay et al., 2006; Ramos et al., 2014) to around 30° inclination that we see today (Cahill and Isacks, 1992). According to Gudnason et al. (2012) and Søager et al. (2013), Nevado and Northern Segment volcanism progressed northwards as the slab warped down starting in the southern Nevado volcanic field in the Late Pliocene–Early Pleistocene and reaching 34°N in the Late Pleistocene where volcanism continued until c. 50 ka before now. The OIB-type volcanism in the Quaternary progressed from southern Payenia at Auca Mahuida (c.1.8–0.9 Ma) via Río Colorado (1.3–0.3 Ma) to Payún Matrú (since c. 0.4) (Germa et al., 2010; Gudnason et al., 2012; Kay et al., 2013; Marchetti et al., 2014; and references therein). Dated rocks from Llancanelo range from 1.0 to around 0.1 Ma, but even younger eruptions may have taken place (Dyhr et al., 2013b; Espanon et al., 2014b; Gudnason et al., 2012). Alkaline volcanism in Nevado and Northern Segment thus progressed northwards probably slightly before the OIB-type magmatism, which also moved northwards further south along a slightly more westerly track from Auca Mahuida via Río Colorado to Payún Matrú. Because many OIB-type magmas in the Río Colorado volcanic field show no indication of subduction zone input, and as less wet melting is indicated for the Papagayos mantle source of the Nevado and Northern Segment magmas relative to the SVZ arc, the implication is that the subducting slab did not supply much enrichment to the Nevado–Northern Segment mantle at the time of magma generation, and that enrichment could mainly have been acquired earlier.

In the Late Miocene, the shallow subduction of the Nazca plate moved arc-type volcanism to the eastern Payenia (e.g. Dyhr et al., 2013b; Litvak et al., 2015; Ramos et al., 2014). The magma generation rate was much lower than in the present day arc as judged by the scarcity of volcanism, probably caused by a much longer distance travelled by the shallowly subducting plate and a broader arc zone. Because the release of fluids beneath the Payenia region was low, and because the mantle wedge temperature may have been lower due to the diminished thickness of the mantle wedge between the relatively cold plates, subducted UCC may have yielded melts by incomplete melting with residual zircon, the UCC-Zr melts. We propose, that rising low-Zr silicic melts reacted with wedge peridotite and the depleted lowermost lithospheric mantle in a manner as proposed by Straub et al. (2011) forming the Papagayos mantle. Because the amount of added UCC-Zr melt was restricted to 1–2%, the mantle was still dominantly peridotitic, and by cooling in the shallow subduction environment it was in effect added to the bottom of the lithosphere of the upper plate. During the steepening of the Nazca plate progressing northwards under Payenia in the Pliocene–Pleistocene, vigorous asthenospheric upwelling of Reyunos/Río Colorado mantle from the south and east may have caused heating of the newly added lowermost lithosphere and the metasomatized wedge mantle. These mantle sources mingled and yielded Nevado and Northern Segment magmas as a mixture of Papagayos and Reyunos melts. Extensional faulting caused by the relaxation of the crust (Folguera et al., 2009) could have enhanced melting as also envisaged as wet spot melting by Kay et al. (2004). Furthermore, small amounts of fluids must have come off the slab as it steepened, metasomatizing the Río Colorado/Reyunos mantle, as represented by the Llancanelo magmas with a small fluid-borne component but with no evidence for involvement of Papagayos mantle. The small slab component also found in the Late Pleistocene to Holocene Payún Matrú magmas (Espanon et al., 2014a; Søager and Holm, 2013; Søager et al., 2013, 2015a) indicates that this is still the case today.

6. Conclusions

1. The late Pleistocene Northern Segment Volcanic Field of the Payenia backarc has olivine phyric primitive alkali basalts with a subduction zone type of incompatible element pattern that expand the Nevado Volcanic Field in Sr, Nd and Pb isotope compositions, and together they span the gap between the Transitional Southern Volcanic Zone magmas and the OIB-type magmas of the southern Payenia backarc.
2. Incompatible trace element ratios such as Ba/Th, Sr/Nd and Eu/Eu* demonstrate that the sources of the subduction zone enriched backarc magmas were enriched by both hydrous fluids and upper continental crustal material. Chile Trench sediments appear not to have contributed significantly to the magmas. The pre-metasomatic mantle ranged from highly depleted (Papagayos end-member) to undepleted mantle (Reyunos end-member).
3. The crustal enrichment of the Papagayos end-member mantle was by melts derived from young upper continental crust with residual zircon, whereas the Reyunos end-member has origin in upwelling Río Colorado OIB-type mantle.
4. The Papagayos mantle is indicated to also be a component in frontal arc magmas of the Transitional Southern Volcanic Zone at Resolana (at Azufre) and thus a mantle end-member for TSVZ together with the two predominant Antuco and Infernillo end-members.
5. Lack of a Pacific MORB isotopic component in the Southern Volcanic Zone arc and backarc from the subducting Nazca plate in combination with the presence of a clear South Atlantic MORB-type component is suggested to be caused by acquisition of the trace element and isotopic composition of the fluids by interaction with the wedge mantle.
6. Our scenario for melting in the subduction zone enriched backarc is correlated to the Pleistocene downwarping of the formerly shallowly subducting Nazca plate. Papagayos type mantle was generated in the mantle wedge during relatively cold conditions during Miocene shallow subduction, and later magmas were derived by means of vigorous inflow of Río Colorado/Reyunos asthenosphere and its heating effect during the Pleistocene steepening of the subducting slab. Partial melting was probably further enhanced by the fluid release from the downwarping plate.

Acknowledgements

We enjoyed the company of F. Brandt in the field, and are grateful for the ICP-MS analyses by J. Kystol at GEUS, as well as for the maintenance of the TIMS in Copenhagen by T. Leeper. We are also grateful to Anders Scherstén, Lawrence Page and Anne Pedersen for the Ar analyses performed in Lund. Discussions with Frederik Brandt, Josephine Persson, Nathali Thorup and Anne Pedersen as well as numerous others, are very much appreciated. The thorough and helpful reviews of two anonymous reviewers are much appreciated. The Danish Research Council for Nature and Universe supported the project by a grant to PMH

[grant no. 12-127010]. NS acknowledges support of the Danish Council for Independent Research [grant no. 0602-02528B to N.S.] and GEOMAR Helmholtz Center for Ocean Sciences, Kiel.

Appendix. Supplementary data

Supplementary data to this article can be found online at http://dx.doi.org/10.1016/j.lithos.2016.06.029.

References

Baker, J., Peate, D., Waight, T., Meyzen, C., 2004. Pb isotopic analysis of standards and samples using a ^{207}Pb–^{204}Pb and thallium to correct for mass bias with a double-focusing MC-ICP-MS. Chemical Geology 211, 275–303.

Bermúdez, A., Delpino, D., Frey, F., Saal, A., 1993. Los Basaltos de Retroarco Extraandinos. In: Ramos, V.A. (Ed.), Geología Y Recursos Naturales de Mendoza. Relatorio I(13), pp. 161–172.

Bertotto, G.W., Cingolani, C.A., Bjerg, E.A., 2009. Geochemical variations in Cenozoic backarc basalts at the border of La Pampa and Mendoza provinces, Argentina. Journal of South American Earth Sciences 28, 360–373.

Brenan, J.M., Shaw, H.F., Ryerson, F.J., Phinney, D.L., 1995. Mineral-aqueous fluid partitioning of trace elements at 900o and 2.0 GPa: constraints on the trace element chemistry of mantle and deep crustal fluids. Geochimica et Cosmochimica Acta 59, 3331–3350.

Burd, A.I., Booker, J.R., Mackie, R., Favetto, A., Pomposiello, M.C., 2014. Three-dimensional electrical conductivity in the mantle beneath the Payún Matrú volcanic field in the Andean backarc of Argentina near 36.5oS: evidence for decapitation of a mantle plume by resurgent upper mantle shear during slab steepening. Geophysical Journal International 198, 812–827.

Cahill, T.A., Isacks, B.L., 1992. Seismicity and shape of the subducted Nazca plate. Journal of Geophysical Research 97 (B12), 17,503–17,529.

Chauvel, C., Blichert-Toft, J., 2001. A hafnium isotope and trace element perspective on melting of the depleted mantle. Earth and Planetary Science Letters 190, 137–151.

DePaolo, D.J., 1981. Trace element and isotopic effects of combined wallrock assimilation and fractional crystallization. Earth and Planetary Science Letters 53, 189–202.

Dyhr, C.T., Holm, P.M., Llambías, E.J., Scherstén, A., 2013a. Subduction controls on Miocene backarc lavas from Sierra de Huantraico and La Matancilla and new $^{40}Ar/^{39}Ar$ dating from the Mendoza region, Argentina. Lithos 179, 67–83.

Dyhr, C.T., Holm, P.M., Llambías, E.J., 2013b. Geochemical constraints on the relationship between the Miocene–Pliocene volcanism and tectonics in the Palaoco and Fortunoso volcanic fields, Mendoza region, Argentina: new insights from $^{40}Ar/^{39}Ar$ dating, Sr–Nd–Pb isotopes and trace elements. Journal of Volcanology and Geothermal Research 266, 50–68.

El Korh, A., Schmidt, S.T., Ulianov, A., Potel, S., 2009. Trace element partitioning in HP-LT metamorphic assemblages during subduction-related metamorphism, Ile de Groix, France: a detailed LA-ICPMS study. Journal of Petrology 50, 1107–1148.

Espanon, V.R., Chivas, A.R., Kinsley, L.P.J., Dossetto, A., 2014a. Geochemical Variations in the Quaternary Andean Back-arc Volcanism, Southern Mendoza, Arge.

Espanon, V.R., Honda, M., Chivas, A.R., 2014b. Cosmogenic 3He and 21Ne surface exposure dating of young basalts from Southern Mendoza, Argentina. Quaternary Geochronology 19, 76–86 (ntina. Lithos 208–209, 251–264).

Ewart, A., Griffin, W.L., 1994. Application of proton-microprobe data to trace-element partitioning in volcanic rocks. Chemical Geology 117, 251–284.

Folguera, A., Naranjo, J.A., Orihashi, Y., Sumino, H., Nagao, K., Polanco, E., Ramos, V.A., 2009. Retroarc volcanism in the northern San Rafael block (34°–35°30′S), southern Central Andes: occurrence, age and tectonic setting. Journal of Volcanology and Geothermal Research 186, 169–185.

Frey, F.A., Nobre Silva, I.G., Huang, S., Pringle, M.S., Meleney, P.R., Weis, D., 2015. Depleted components in the source of hotspot magmas: evidence from the ninety east ridge (Kerguelen). Earth and Planetary Science Letters 426, 293–304.

Gaetani, G.A., Grove, T.L., 2003. Experimental constraints on the melt generation in the mantle wedge. In: Eiler, J.M. (Ed.), Inside the Subduction Factory. Geophysical Monograph, American Geophysical Union vol. 138, pp. 107–134.

Germa, A., Quidelleur, X., Gillot, P.Y., Tchilinguirian, P., 2010. Volcanic evolution of the backarc Pleistocene Payún Matrú volcanic field (Argentina). Journal of South American Earth Sciences 29, 717–730.

Grove, T.L., Till, C.B., Lev, E., Chatterljee, N., M'dard, E., 2009. Kinematic variables and water transport control the formation and location of arc volcanoes. Nature 459, 694–697.

Gudnason, J., Holm, P.M., Søager, N., Llambías, E.J., 2012. Geochronology of the late Pliocene to recent volcanic activity in the Payenia back-arc volcanic province, Mendoza, Argentina. Journal of South American Earth Sciences 37, 191–201.

Handley, H.K., Turner, S., Macpherson, C.G., Gertisser, R., Davidson, J.P., 2011. Hf–Nd isotope and trace element constraints on subduction inputs at island arcs: limitations of Hf anomalies as sediment input indicators. Earth and Planetary Science Letters 304, 212–223.

Hermann, J., Rubatto, D., 2009. Accessory phase control on the trace element signature of sediment melts in subduction zones. Chemical Geology 265, 512–526.

Hernando, I.R., Llambías, E.J., González, P.D., Sato, K., 2012. Volcanic stratigraphy and evidence of magma mixing in the Quaternary Payun Matru volcano, Andean backarc in western Argentina. Andean Geology 39, 158–179.

Hill, E., Blundy, J.D., Wood, B.J., 2011. Clinopyroxene-melt trace elements partitioning and the development of a predictive model for HFSE and Sc. Contributions to Mineralogy and Petrology 161, 423–438.

Hirose, K., 1997. Melting experiments on lherzolite KLB-1 under hydrous conditions and generation of high-magnesian andesitic melts. Geology 25, 42–44.

Holm, P.M., Søager, N., Dyhr, C.T., Nielsen, M.R., 2014. Enrichments of the mantle sources beneath the Southern Volcanic Zone (Andes) by fluids and melts derived from abraded upper continental crust. Contributions to Mineralogy and Petrology 167, 1004. http://dx.doi.org/10.1007/s00410-014-1004.

Irvine, T.N., Baragar, W.R.A., 1971. A guide to the chemical classification of common volcanic rocks. Canadian Journal of Earth Sciences 8, 523–548.

Jacques, G., Hoernle, K., Gill, J., Hauff, F., Wehrmann, H., Garbe-Schönberg, D., van den Bogaard, P., Bindeman, I., Lara., L.E., 2013. Across-arc geochemical variations in the Southern Volcanic Zone, Chile (34.5–38.0°S): constraints on mantle wedge and slab input compositions. Geochimica et Cosmochimica Acta 123, 218–243.

Jochum, K.P., Nehring, F., 2006. GeoReM preferred values. Max-Plank-Institut für Chemie, 11/2006. http://georem.mpch-mainz.gwdg.de.

Kay, S.M., Gorring, M., Ramos, V.A., 2004. Magmatic sources, setting, and causes of Eocene to Recent Patagonian plateau magmatism (36 degrees S to 52 degrees S latitude). Revista de la Asociación Geológica Argentina 59 (4), 556–568.

Kay, S.M., Godoy, E., Kurtz, A., 2005. Episodic arc migration, crustal thickening, subduction erosion, and magmatism in the south-Central Andes. Geological Society of America Bulletin 117, 67–88.

Kay, S.M., Burns, W.M., Copeland, P., Mancilla, O., 2006. Upper Cretaceous to Holocene magmatism and evidence for transient Miocene shallowing of the Andean subduction zone under the northern Neuquén Basin. Geological Society of America, Special Paper 407, 19–60.

Kay, S.M., Jones, H.A., Kay, R.W., 2013. Origin of Tertiary to Recent EM- and subduction-like chemical and isotopic signatures in Auca Mahuida region (37–38°S) and other Patagonian plateau lavas. Contributions to Mineralogy and Petrology 166, 165–192.

Kendrick, E., Bevis, M., Smalley Jr., R., Brooks, B., Vargas, R.B., Lauria, E., Souto, L.P., 2003. The Nazca-South America Euler vector and its rate of change. Journal of South American Earth Sciences 16, 125–131.

Kessel, R., Schmidt, M.W., Ulmer, P., Pettke, T., 2005. Trace element signature of subduction-zone fluids, melts and supercritical liquids at 120–180 km depth. Nature 437, 724–727.

Klemme, S., Prowatke, S., Hametner, K., Günther, D., 2005. Partitioning of trace elements between rutile and silicate melts: implications for subduction zones. Geochimica et Cosmochimica Acta 69, 2361–2371.

Kogiso, T., Tatsumi, Y., Nakano, S., 1997. Trace element transport during dehydration processes in the subducted oceanic crust: 1. Experiments and implications for the origin of ocean island basalts. Earth and Planetary Science Letters 148, 193–205.

Litvak, V.D., Spagnuolo, M.G., Folguera, A., Poma, S., Jones, R.E., Ramos, V.A., 2015. Late Cenozoic calc-alkaline volcanism over the Payenia shallow subduction zone, South-Central Andean back-arc (34°30′–37°S), Argentina. Journal of South American Earth Sciences 64, 365–380.

Lucassen, F., Trumbull, R., Franz, G., Creixell, C., Vásquez, P., Romer, R.L., Figueroa, O., 2004. Distinguishing crustal recycling and juvenile additions at active continental margins: the Paleozoic to recent compositional evolution of the Chilean Pacific margin (36–41°S). Journal of South American Earth Sciences 17, 103–119.

Lucassen, F., Wiedicke, M., Franz, G., 2010. Complete recycling of a magmatic arc: evidence from chemical and isotopic composition of Quaternary trench sediments in Chile (36°–40°S). International Journal of Earth Sciences 99, 687–701.

Marchetti, D.W., Hynek, S.A., Cerling, T.E., 2014. Cosmogenic 3He exposure ages of basalt flows in the northwestern Payún Matru volcanic field, Mendoza Province, Argentina. Quaternary Geochronology 19, 67–75.

Marshall, H.R., Schumacher, J.C., 2012. Arc magmas sourced from mélange diapirs in subduction zones. Nature Geoscience. http://dx.doi.org/10.1038/NGEO1634.

Pearce, J.A., Kempton, P.D., Nowell, G.M., Noble, S.R., 1999. Hf–Nd element and isotope perspective on the nature and provenance of mantle and subduction components in western Pacific Arc-basin systems. Journal of Petrology 40, 1579–1611.

Plank, T., Langmuir, C.H., 1993. Tracing trace elements from sediment input to volcanic output at subduction zones. Nature 362, 739–743.

Ramos, V.A., Litvak, V.D., Folguera, A., Spagnuolo, M., 2014. An Andean tectonic cycle: from crustal thickening to extension in a thin crust (34°–37°_SL). Geoscience Frontiers 5, 351–367. http://dx.doi.org/10.1016/j.gsf.2013.12.009.

Rodríguez, C., Sellés, D., Duncan, M., Langmuir, C., Leeman, W., 2007. Adakitic Dacites formed by intracrustal crystal fractionation of water-rich parent magmas at Nevado de Longaví volcano (36.2°S; Andean southern volcanic zone, Central Chile). Journal of Petrology 48, 2033–2061.

Rubatto, D., Hermann, J., 2003. Zircon formation during fluid circulation in eclogites (Monviso, Western Alps): implications for Zr and Hf budget in subduction zones. Geochimica et Cosmochimica Acta 67, 2173–2187.

Rubatto, D., Hermann, J., 2007. Experimental zircon/melt and zircon/garnet trace element partitioning and implications for the geochronology of crustal rocks. Chemical Geology 241, 38–61.

Rudnick, R.L., Gao, S., 2003. Composition of the continental crust. In: Carlson, R.W., Holland, H.D., Turekian, K.K. (Eds.), Treatise on Geochemistry: The Crust. Elsevier, pp. 1–64.

Salters, V.J.M., Stracke, A., 2004. Composition of the depleted mantle. Geochemistry, Geophysics, Geosystems 5. http://dx.doi.org/10.1029/2003GC000597.

Scambelluri, M., Pettke, T., Rampone, E., Godard, M., Reusser, E., 2014. Petrology and trace element budgets of high-pressure peridotites indicate subduction dehydration of serpentinized mantle (Cima di Gagnone, Central Alps, Switzerland). Journal of Petrology 55, 459–498.

Sellés, D., Rodríguez, A.C., Duncan, M., Naranjo, J.A., Gardeweg, M., 2004. Geochemistry of Nevado de Longaví volcano (36.2°S): a compositionally atypical arc volcano in the Southern Volcanic Zone of the Andes. Revista Geologica de Chile 31, 293–315.

Søager, N., Holm, P.M., 2013. Melt-peridotite reactions in upwelling EM1-type eclogite bodies: constraints from alkaline basalts in Payenia, Argentina. Chemical Geology 360-361, 204–219.
Søager, N., Holm, P.M., Llambías, E.J., 2013. Payenia volcanic province, southern Mendoza, Argentina: OIB mantle upwelling in a backarc environment. Chemical Geology 349-350, 36–53.
Søager, N., Holm, P.M., Thirlwall, M.F., 2015a. Sr, Nd, Pb and Hf isotopic constraints on mantle sources and crustal contaminants in the Payenia volcanic province, Argentina. Lithos 360-361, 204–219.
Søager, N., Portnyagin, M., Hoernle, K., Holm, P.M., Hauff, F., Garbe-Schönberg, 2015b. Olivine major and trace element compositions in southern Payenia basalts, Argentina: evidence for pyroxenite peridotite melt mixing in a backarc setting. Journal of Petrology 56, 1495–1518.
Spandler, C., Pettke, T., Hermann, J., 2014. Experimental study of trace element release during ultrahigh-pressure serpentinite dehydration. Earth and Planetary Science Letters 391, 296–306.
Stepanov, A.S., Hermann, J., Rubatto, D., Rapp, R.P., 2012. Experimental study of monazite/melt partitioning with implications for the REE, Th and U geochemistry of crustal rocks. Chemical Geology 300-301, 200–220.
Stern, C.R., 1991. Role of subduction erosion in the generation of the Andean magmas. Geology 19, 78–81.
Stern, C.R., 2004. Active Andean volcanism: its geologic and tectonic setting. Revista Geologica de Chile 31, 161–206.
Straub, S.M., Gomez-Tuena, A., Stuart, F.M., Zellmer, G.F., Espinasa-Perena, R., Cai, M.Y., Iizuka, Y., 2011. Formation of hybrid arc andesites beneath thick continental crust. Earth and Planetary Science Letters 303, 337–347.
Sun, S.-S., McDonough, W.F., 1989. Chemical and isotopic systematics of oceanic basalts: implications for mantle composition and processes. Geological Society of London, Special Publication 42, 313–345.
Tassara, A., Götze, H.J., Schmidt, S., Hackney, R., 2006. Three-dimensional density model of the Nazca plate and the Andean continental margin. Journal of Geophysical Research 111 (B09404). http://dx.doi.org/10.1029/2005JB003976.
Tatsumi, Y., Kogiso, T., 2003. The subduction factory: its role in the evolution of the Earth's crust and mantle. Geological Society of London, Special Publication 219, 55–80.
Taylor, S.R., McLennan, S.M., 1985. The Continental Crust: Its Composition and Evolution. Blackwell, Oxford.
Tebbens, S.F., Cande, S.C., 1997. Southeast Pacific tectonic evolution from early Oligocene to Present. Journal of Geophysical Research 102, 12061–12084.
Thirlwall, M.F., 2000. Inter-laboratory and other errors in Pb isotope analyses investigated using a ^{207}Pb–^{204}Pb double spike. Chemical Geology 163, 299–322.
Thirlwall, M.F., Smith, T.E., Graham, A.M., Theodorou, N., Hollings, P., Davidson, J.P., Arculus, R.J., 1994. High field strength element anomalies in arc lavas: source or process? Journal of Petrology 35, 819–838.
Völker, D., Wehrmann, H., Kutterolf, S., Iyer, K., Rabbel, W., Geersen, J., Hoernle, K., 2014. Constraining input and output fluxes of the southern-central Chile subduction zone: water, chlorine and sulfur. International Journal of Earth Sciences 103, 2129–2153.
Workman, R.K., Hart, S.R., 2005. Major and trace element composition of the depleted mantle. Earth and Planetary Science Letters 231, 53–72.
Xiao, Y., Lavis, S., Niu, Y., Pearce, J.A., Wang, H.L.H., Davidson, J., 2012. Trace-element transport during subduction-zone ultrahigh-pressure metamorphism: evidence from western Tianshan, China. Geological Society of America Bulletin 124, 1113–1129.